9-10-2019

Structure-function relationship in S-nitrosoglutathione reductase and the development of fluorogenic pseudo-substrates

Nneamaka Chinwendu Onukwue
University of Windsor

**Structure-function relationship in S-nitrosoglutathione reductase and the
development of fluorogenic pseudo-substrates**

By

Nneamaka Chinwendu Onukwue

A Thesis
Submitted to the Faculty of Graduate Studies
through the Department of Chemistry and Biochemistry
in Partial Fulfillment of the Requirements for
the Degree of Master of Science
at the University of Windsor

Windsor, Ontario, Canada

2019

Structure-function relationship in S-nitrosoglutathione reductase and the development of fluorogenic pseudo-substrates

by

Nneamaka Chinwendu Onukwue

APPROVED BY:

_____

J. Hudson

Department of Biomedical Sciences

_____

D. Marquardt

Department of Chemistry & Biochemistry

_____

B. Mutus, Advisor

Department of Chemistry & Biochemistry

September 10, 2019

DECLARATION OF ORIGINALITY

I hereby certify that I am the sole author of this thesis and that no part of this thesis has been published or submitted for publication.

I certify that, to the best of my knowledge, my thesis does not infringe upon anyone's copyright nor violate any proprietary rights and that any ideas, techniques, quotations, or any other material from the work of other people included in my thesis, published or otherwise, are fully acknowledged in accordance with the standard referencing practices. Furthermore, to the extent that I have included copyrighted material that surpasses the bounds of fair dealing within the meaning of the Canada Copyright Act, I certify that I have obtained a written permission from the copyright owner(s) to include such material(s) in my thesis and have included copies of such copyright clearances to my appendix.

I declare that this is a true copy of my thesis, including any final revisions, as approved by my thesis committee and the Graduate Studies office, and that this thesis has not been submitted for a higher degree to any other University or Institution.

ABSTRACT

S-nitrosation is the attachment of a nitric oxide moiety to the thiol side chain of cysteine. S-nitrosoglutathione (GSNO) acts as a bioactive reservoir for NO to maintain an equilibrium in the concentration of NO in the body. Due to this, the study of the enzyme S-nitrosoglutathione reductase has of great interest because of its ability to metabolize GSNO. S-nitrosoglutathione reductase's activity has been linked to a number of human diseases. Chapter 1 of this thesis presents a proposed allosteric binding domain on GSNOR. Positive cooperativity (sigmoidal deviation) was observed from steady state analysis of GSNOR which indicated an affinity for the binding of GSNO at this site. The presence of such a site was further supported by Molecular docking simulations and HDX-MS which showed that the amino acids Gly321, Lys323, Asn185 and Lys188 interact with molecules bound at this site.

Chapter two introduces four reagents that can function as probes or pseudo-substrates for the monitoring of enzymatic activity as well as measuring concentrations of free thiols in vitro and live cells. These reagents are *N,N*-di(thioamido-fluoresceinyl)-cystine (DTFCys$_2$), *N,N*-di(thioamido-fluoresceinyl)-homocystine (DTFHCys$_2$), *N*-amido-*O*-aminobenzoyl-*S*-nitrosoglutathione (AOASNOG), and *N*-thioamido-fluoresceinyl-*S*-nitroso-glutathione (TFSNOG). They are easy to prepare and purity and can be used in various applications.

DEDICATION

To my Family.

ACKNOWLEDGEMENTS

TABLE OF CONTENTS

LIST OF TABLES

LIST OF FIGURES

LIST OF ABBREVIATIONS/SYMBOLS

NO	Nitric Oxide
NOS	Nitric Oxide Synthases
nNOS	Neuronal Nitric Oxide Synthases
iNOS	Inducible Nitric Oxide Synthases
eNOS	Endothelial Nitric Oxide Synthases
NADH	nicotinamide adenine dinucleotide phosphate
FAD	Flavin adenine dinucleotide
GSNO	S-nitrosoglutathione
GSNOR	S-nitrosoglutathione reductase
GSH-FDH	Glutathione-dependent formaldehyde dehydrogenase
GSH	Glutathione
GSSG	Glutathione persulfide
NH$_2$OH	Hydroxylamine
Glu	Glutamic acid
Arg	Arginine
Cys	Cysteine
His	Histidine
Asn	Asparagine
Lys	Lysine
2x YT	Yeast extract Tryptone
MS	Mass Spectroscopy
DTT	Dithiothreitol

CHAPTER 1

Proposed Allosteric site on S-nitrosoglutathione Reductase

Chapter summary

S-nitrosoglutathione reductase, an enzyme in the alcohol dehydrogenase family, is responsible for the metabolism of GSNO as well as the detoxification of formaldehyde in the body. Steady state assay of the WT of this enzyme revealed a deviation from the classical Michaelis Menten kinetics, fitting more into a sigmoidal curve. This led to the hypothesis that the enzyme has an allosteric site that binds the substrate GSNO and increases the activity of the enzyme. Molecular docking was used to visualize the possible location of such a site, and it was found adjacent to the structural zinc. Four amino acid residues were implicated to have an interaction with the substrate bound at the site. They are Lys188, Lys323, Asn185 and Gly321. Mutations to the Lysine residues were performed to monitor how the changes to the environment around this site would affect the activity of the enzyme and its affinity for binding the substrate. To further confirm the presence of the proposed allosteric site Hydrogen Deuterium exchange mass spectroscopy was performed. This exchange showed decreased uptake of deuterium by three of the four residues at the proposed site identified on the peptide list. Asn185 was not identified and will be part of the further investigations with respect to this experiment. All results obtained from the steady state analysis and HDX-MS support the hypothesis that there is an allosteric site on the enzyme GSNOR located adjacent to the structural zinc.

1.1 Nitric Oxide

Nitric Oxide (NO) is a diatomic free radical gasotransmitter. It is the first identified gasotransmitter discovered to be the endothelium-derived relaxing factor (EDRF) that is responsible for vascular smooth muscle relaxation. [1-4] NO is a well-established signaling molecule involved in many physiological processes. These include the control of vascular tone and blood pressure, promoting angiogenesis, mediating neurotransmission, immune response, and wound healing.[5] NO is also involved in the regulation of growth, immunity, environmental and root development of Plants.[6]

1.1.1 NO Synthases

NO regulation involves the control of nitric oxide synthases (NOS), a group of enzymes responsible for the biosynthesis of NO. Endogenous NO is enzymatically synthesized in mammalian tissues by three isoforms of NOS. These isoforms are neuronal NOS (nNOS, NOS 1), inducible NOS (iNOS, NOS 2) and endothelial NOS (eNOS, NOS 3) according to basal level of activity and constitutive expression in tissues. NOSs produce NO in eukaryotic cells which are found in animals, and some algae. Other organisms utilize alternative methods such as nitrite reduction in the production of NO.[7-8]

The isoforms of NOS function as homodimers, catalyzing the oxidation of L-arginine to L-citrulline and NO in the presence of molecular oxygen with reduced nicotinamide adenine dinucleotide phosphate (NADPH), as a co-substrate.[9-10] NO productions catalyzed by NOS require a number of cofactors/coenzymes such as flavin adenine dinucleotide (FAD), flavin mononucleotide (FMN), tetrahydrobiopterin (BH4)

3

and calmodulin. [11] nNOS is natively expressed in the neurons of the peripheral and central nervous system, in addition to the epithelial cells of various organs.[12] nNOS activity is Ca^{2+} dependent and NO derived by nNOS mediates synaptic plasticity affecting complex physiological functions [13-14] and is a part of the central regulation of blood pressure.[15-16] iNOS is expressed in the presence of inducing stimulants like cytokines. Once induced, it produces substantial amounts of NO and is completely Ca^{2+} independent. iNOS was discovered in macrophages and is involved in the immune system and inflammatory bowel disease (IBSs).[17-18] eNOS from the name is expressed in the endothelial cells and just like nNOS is Ca^{2+} dependent. NO produced by this isoform results in vasorelaxation and protects blood vessels from thrombosis by the inhibition of platelet adhesion and aggregation.[19-21]

1.1.2 NO signaling Mechanism

There are several NO signaling mechanisms that have been identified. The most common are the classical, nonclassical and less classical mechanisms.[22] Classical signaling involves the activation of soluble guanylate cyclase which then converts guanosine triphosphate (GTP) to cyclic guanosine monophosphate (cGMP). This leads to the activation of cGMP-dependent protein kinases subsequently facilitating down-stream effects. Nonclassical signaling suggests the formation of NO-induced posttranslational modifications (PTMs) such as S-glutathionylation, S-nitrosation and tyrosine nitration. The less classical signaling has important implication for cell respiration and intermediate

metabolism due to the interaction between NO and the mitochondrial cytochrome c oxidase.[23-26]

1.2 Protein S-nitrosation

S-nitrosation is the covalent attachment of a nitric oxide (NO) group to the thiol side chain of the amino acid cysteine resulting in the formation of S-nitrosothiols (SNOs).[27] The post-translational modification of Cysteine residues in proteins has been regarded as a primary mechanism which NO uses to regulate cell signaling.[28-30] S-nitrosation of proteins is not directly catalyzed by enzymes, however protein catalyzed S-nitrosation and denitrosation pathways have been discovered and are yet to be understood in the context of global proteomic analysis.[29] There has been increasing evidence that suggests the participation of S-nitrosation in both normal physiology and pathogenesis of several human diseases.[31] For instance, in GSNOR knockout mice increased levels of SNO-proteins were observed which demonstrates the role of GSNO/GSNOR in SNO-protein homeostasis. First step in S-nitrosation process is NO oxidized to higher oxides of nitrogen such as dinitrogen trioxide (N_2O_3) when reacted with molecular oxygen (O_2). N_2O_3 can react directly with the thiols as shown in equation 1.2.1.

$$RS^- + N_2O_3 \longrightarrow RSNO + NO_2^- \qquad \text{Equation 1.2.1}$$
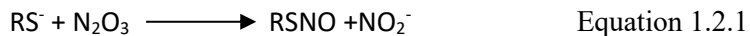
A proposed alternative mechanism for the formation of SNO is the reacting of NO

with reduced thiol forming a radical intermediate.[31] Recent evidence shows that the

reaction of NO with molecular oxygen (O_2) is not only a primary pathway for S-

nitrosation of thiols but might also yield products of thiol oxidation sometimes greater

than RSNOs.[30,32]

S-nitrosation of proteins occurs through transnitrosation. Transnitrosation

reactions are all fully reversible and often include SNOs of low molecular weight

such as GSNO.[29,33]

$$\text{Protein-S}^- + \text{GSNO} \longrightarrow \text{Protein-SNO} + \text{GS}^- \qquad \text{Equation 1.2.2}$$

S-nitrosylation is involved in the physiology and dysfunction of cardiac, airway and

skeletal muscle as well as the immune system showing wide-ranging functions in cell

and tissues.[34-37]

1.3 S-nitrosoglutathione Reductase (GSNOR)

1.3.1 GSNOR as a product of ADH 5

S-nitrosoglutathione Reductase (GSNOR) is an enzyme in the alcohol

dehydrogenase (ADH) family. The alcohol dehydrogenase family has been evolutionarily

conserved from bacteria to man with five distinct classes containing seven known

isoforms.[38] ADH is involved in several important roles in the body but the most studied is

the metabolism of short chain alcohols. GSNOR is a member of the class III alcohol

dehydrogenase family. GSNOR is encoded by the ADH5 gene located on the reverse strand of chromosome 4 (4q23-Chr4: 99,993,567-10,000,985).[38]

GSNOR also known as ADH5, FALDH, GSH-FDH and Formaldehyde dehydrogenase is a ubiquitously expressed NADH dependent enzyme with the ability to oxidize medium-chain alcohols and the GSH adduct S-hydroxymethylglutathione (HMGSH). It also reduces GSNO using NADH as a cofactor producing GSNHOH as an intermediate which can further react with GSH to produce GSSG and NH_2OH. GSNOR when acting as a glutathione-dependent formaldehyde dehydrogenase is critical in the metabolic elimination of formaldehyde (Figure 1.3.1). This formaldehyde is eliminated by reacting with glutathione to produce the adduct S-hydroxymethylglutathione which can then be oxidized to S-formylglutathione. This reaction requires NAD+ as a cofactor which leads to the production of NADH, a cofactor necessary for the metabolism of GSNO.[39-41] GSNOR in plants is important for growth and root development. Most of the studies on GSNOR done on plant are mainly focused on the *Arabidopsis thaliana* plant however, there have been papers published on sunflower (*Helianthus annuus* L.), pepper (*Capsicum annuum* L.), maize and rice.[42] GSNOR in humans can be found in the endometrium, ovary, fat, esophagus, prostate, liver and kidney.[43]
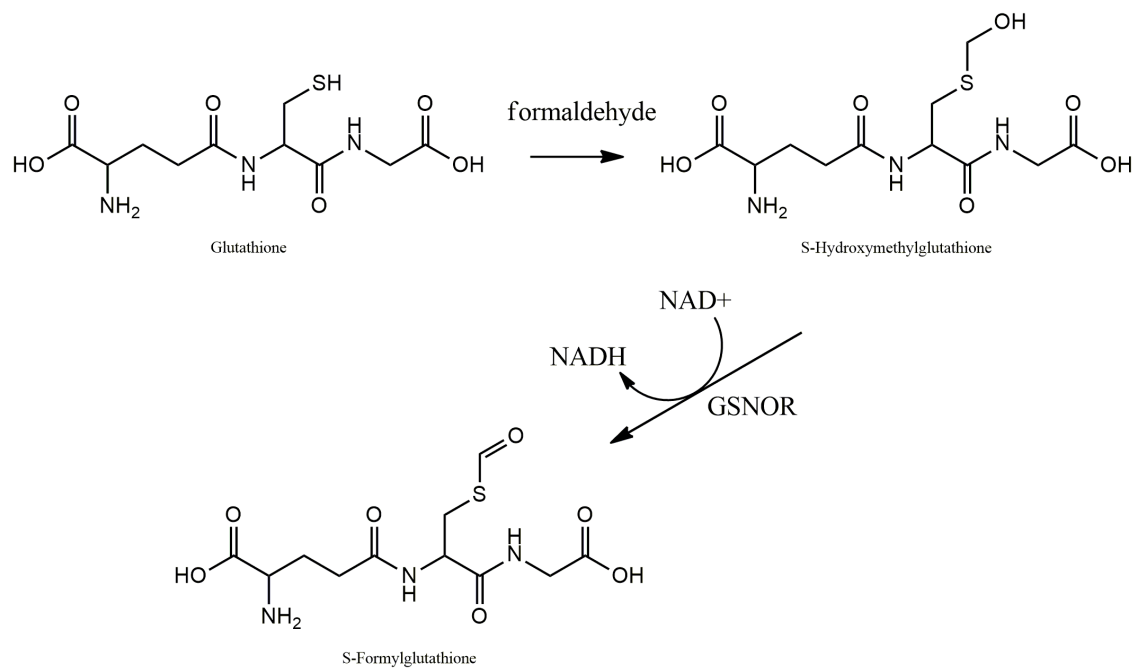
Figure 1.3.1: GSNORs role in the detoxification of formaldehyde. In step 1, glutathione reacts with a formaldehyde at the free thiol group to produce the spontaneous adduct HMGSH. In step 2, HMGSH is oxidized at the S-hydroxymethyl group by GSNOR to S-formylglutathione using NAD+ as a cofactor.

1.3.2. GSNOR protein structure

GSNOR functions as a homodimer with 40kDa subunits containing 347 amino acids per subunit (Figure 1.3.2, page 11). In each subunit there is a catalytic domain and a coenzyme binding domain. GSNOR is a metalloprotein with two zinc atoms per monomer for a total of four zinc atoms per functional enzyme. The zinc atoms are both in the catalytic domain however the catalytic zinc acts as a lewis acid during catalysis while the structural zinc is critical for the maintenance of proper protein structure. GSNOR requires a coenzyme that may vary depending on the substrate. These include NADH, NADPH+H$^+$ and, NAD(P)$^+$.[44]

The amino acid residues involved in the binding of substrates are highly conserved, particularly Glu68 and Arg379 as they are integral to the catalysis mechanism.[45,46] The catalytic zinc is coordinated by the residues Cys45, His67, Cys174 and Glu68 or a water molecule. Similarly, the structural zinc is coordinated by four closely spaced cysteine residues Cys97, Cys100, Cys103 and Cys111.[47,48] Although the structural zinc is not involved in the catalytic mechanism mutations to any of the cysteine residues results in the enzymes inactivity. The catalytic domain moves towards the coenzyme binding domain during the formation of the complex HMGSH with NADH present.

We hypothesize the presence of an allosteric site on GSNOR that binds the substrate GSNO and enhances the activity of the enzyme. This site is postulated to be localized in a cleft adjacent to the structural zinc atom. Four amino acid residues in this

local with molecules bound at this site. The amino acid residues involved are Lys323, Gly321, Asn185 and Lys188 with both Lysine residues proposed to interact indirectly with molecules while the Glycine and Asparagine residues interact directly with bound molecules. This was Supported by molecular docking (MD) simulations performed on the enzyme and the substrate GSNO.
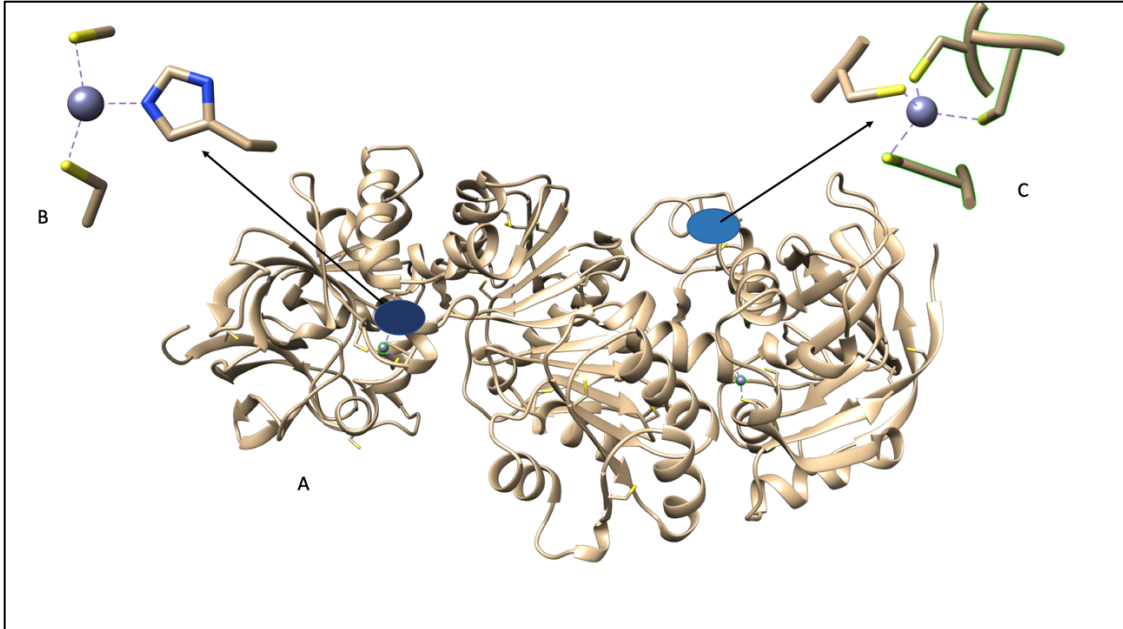
Figure 1.3.2 GSNOR crystal structure showing the 40kDa subunits. (A) the enzyme structure showing the four zinc atoms. The active site is located in the cleft between the catalytic zinc and the structural zinc. (B) shows the catalytic zinc coordinated by two of the three Cysteine residues and the Histidine. (C) shows the structural zinc coordinated by the four Cysteine residue in close proximity of each other were two of the residues make up the CXXC motif of the Enzyme.

1.3.3. Functions of GSNOR

GSNOR as previously mentioned is highly conserved in eukaryotic and prokaryotic organisms and expressed in all tissues studied.[49,50] Multiple studies have provided documentation of the involvement of GSNOR in a number of pathways from metabolism of GSNO,[51-55] to w-hydroxy fatty acid oxidation,[56,57] and formaldehyde detoxification.[58-61] The most characterized and studied functions of GSNOR are the glutathione-dependent formaldehyde oxidation and the NADH-dependent GSNO reduction (fig 1.3.1 and fig 1.3.3). The glutathione-dependent formaldehyde dehydrogenase activity is important for the elimination of formaldehyde, a classified carcinogen because of its high reactivity with DNA and proteins.[62] Studies have shown that GSNOR is localized in the cytoplasm and as a condensed chromatin in the nucleus,[63] this supports its function in the elimination of formaldehyde and protecting DNA from its toxicity.

The substrates that are preferred by GSNOR are HMGSH and GSNO. However, GSNO is considered the best substrate due to its catalytic efficiency of metabolism being twice that of HMGSH.[64] GSNO is metabolized by the reductase activity of GSNOR with the first step being the reduction of GSNO in the presence of the NADH to the unstable intermediate glutathione N-hydroxysulfenamide (GSNHOH). In the presence of excess GSH in the system, GSNHOH will react with the GSH to produce a glutathione dimer (GSSG) and a side product of Hydroxylamine (NH_2OH) (Figure 1.3.3). When no GSH is present the reaction can go in a different direction with GSNHOH spontaneously forming

glutathione sulfonamide ($GSNONH_2$) which can then be hydrolyzed under acidic conditions to glutathione sulfonic acid (GSOOH) and ammonia (NH_4^+). The above reaction schemes are all irreversible.

Under physiological conditions, the ratio of $NADH/NAD^+$ present is typically low.[65] This is not favorable for reductive pathways that require NADH implying that the reductase activity of GSNOR may depend on the availability of the cofactor. An increase in cellular NADH levels can be triggered by various factors like the inhibition of NADH dehydrogenase.[66] GSNOR deficient mice exhibit substantial increases in protein s-nitrosation.[67] In the cellular environment GSNO is observed to be in equilibrium with S-nitrosated proteins via reversible transnitrosation, while the observation of increased levels of S-nitrosation places GSNOR in a crucial role for the maintenance of SNO homeostasis by reducing GSNO.

Figure 1.3.3 Reaction scheme showing how GSNOR works. (A) shows the process by which the substrate GSNO is metabolized by the enzyme GSNOR in the presence of the cofactor NADH to the unstable intermediate GSNHOH. (B) GSNHOH in the presence of excess GSH will react further to produce GSSG. (C) When there is no GSH present GSNHOH spontaneous produces GSONH2 which can be further hydrolyzed to produce Glutathione sulfuric acid and Ammonia

1.3.4. Physiology and Inhibitors of GSNOR

GSNOR plays a crucial role in the variation of NO in the cells. NO is highly reactive and will form stable RSNO equilibrium in the presence of GSH in the form of GSNO, a reservoir of bioavailable NO. NO and by extension GSNO plays a critical role in the relaxation of smooth muscle,[68-70] cardiopulmonary regulation[71-73], and several other intra/extracellular functions.[74] GSNOR dysregulation has been implicated in numerous diseases such as asthma, cystic fibrosis and intestinal lung disease. GSNOR knockout mice have been used to obtain valuable data related to GSNOR function. Canonical NO-mediated pathways and RSNO levels are severely modified when GSNOR activity is modulated. GSNOR plays an important protective role in the immune system's development of lymphocytes. GSNOR knockout mice show a decrease in CD4 thymocyte development and an increase in lymphocytic apoptosis.[75] GSNOR's regulation activity in the brain affects a broad swath of cellular functions ranging from neural development to other neurodegenerative diseases seen in adults.

GSNO has been identified as a long-lived and potent relaxant of human airway in pulmonary physiology, due to its role as a reservoir for NO. This is characterized by inflammation and hyper-responsiveness in the airway.[76] GSNO has been linked to other diseases like IBS, autoimmune encephalomyelitis and more. An increase in SNO levels in knockout mice with asthma lead to the study of therapeutic approaches for the inhibition of GSNOR activity to restore SNO levels. Investigations into inhibitors of GSNOR are on-going to aid patients affected by some of the diseases. The most productive progress

in the regulation of GSNOR is the development of N9115, an inhibitor marketed as Cavosonstat, that assists cystic fibrosis (CF) patients with the ΔF508-CFTR mutation. This mutation occurs within the gene for the cystic fibrosis transmembrane conductance regulator (CFTR) and accounts for most of cases of CF.[77,78] N91115 ensures the availability of GSNO to promote CFTR development and plasma membrane stability via its inhibition of GSNOR.

1.4 Computational study of the proposed allosteric site

A computational study of the enzyme to identify the location of the proposed allosteric site via the measurement of minimum energy between the substrate and the enzyme was conducted using molecular docking simulations. This study was done as a collaboration between Sahar Nikoo, Dr. James Gauld, Dr. Bei Sun, and Dr. Bulent Mutus. The crystal structure for GSNOR utilized was obtained from the PDB library (ID:3QJ5) and was loaded onto the Molecular Environment Software (MOE). This study revealed that at the speculated site, the bound ligand interacts with four amino acid residues. These are lysine188, lysine323, glycine321 and asparagine185 (Figure 1.4). The docking results showed that when GSNO is bound at the proposed site, it interacts directly with the residues Gly321 and Asn185. The results also show that Lys188 and Lys323 interact with GSNO via a solvent network of hydrogen bonds.[5] Docking scores obtained from this study show a score of -8.60 when GSNO is bound to the known active site of the enzyme and a score of -10.4 when GSNO binds to the postulated allosteric site. Docking scores are used to predict the binding affinity of a molecule with a low score

showing the system is stable and shows the interaction is favorable. This study further confirms the presence of the proposed allosteric binding site for the substrate GSNO.
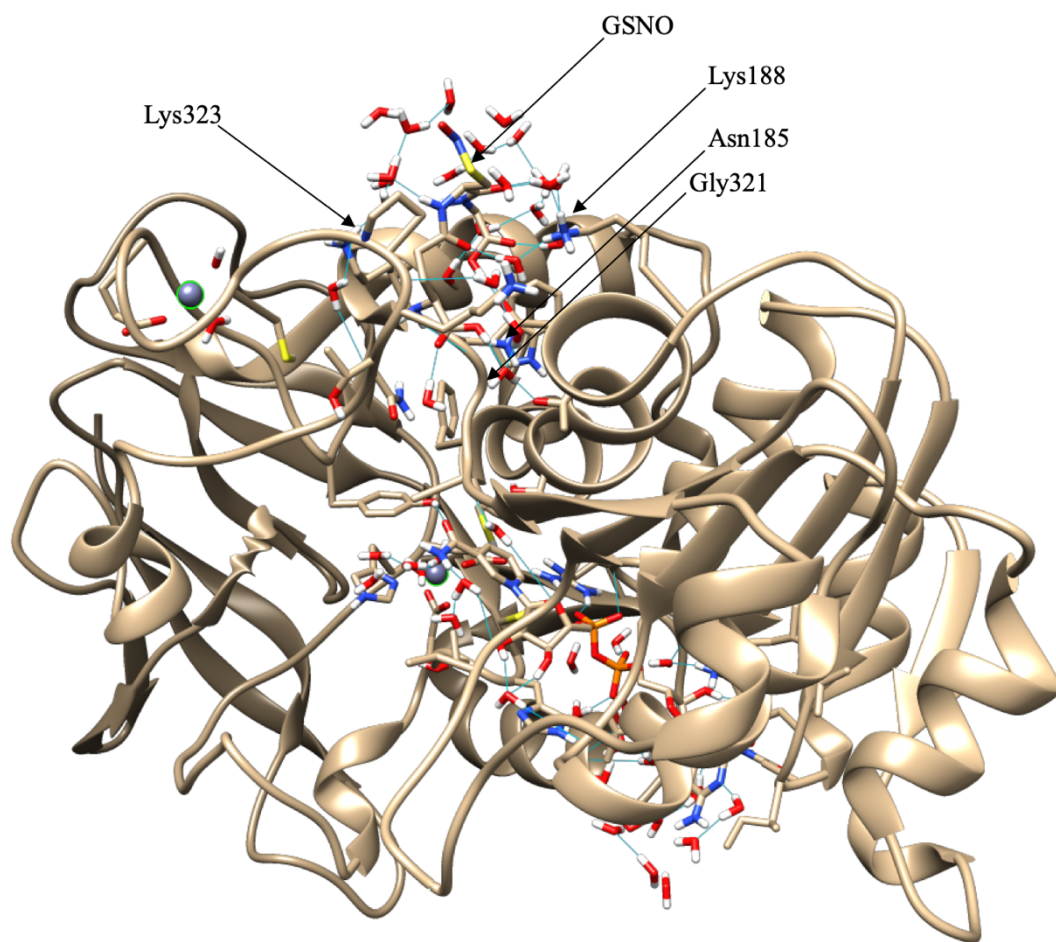
Figure 1.4 Molecular docking simulation showing the location of the proposed allosteric site and how when GSNO is bound it interacts with the implicated residues direct or via the solvent network of hydrogen bonds. The interactions via hydrogen bonds are shown by the blue lines.

1.5 Hydrogen deuterium exchange (HDX) MS

A Hydrogen deuterium exchange experiment was carried out using a Synapt G1

that was properly fitted with custom TRESI apparatus as per Wilson *et al.*[53] The reagents

used for this are reported in appendix B from the work done by Kathleen Fontana. The

experiment was performed using 5- and 10-mm reaction spaces corresponding to 2 and 4

seconds, respectively. Data collection was done in IMS mode within the range of 400-

1500 m/z. Experimental uptake of deuterium for each peptide was calculated using a

software that was custom-built for this purpose. Data was collected on the same day for

all trials. These include 5-minute spectrums of GSNOR without deuterium exchange,

with two- and four-seconds exchanges. This was followed by 5 min spectrums of

GSNOR + 20x GSNO (excess) with the same conditions as mentioned above.

1.5.1 (HDX) MS Results

The results from the HDX experiments seen in Appendix B supports the presence

of the proposed allosteric binding site. The incorporation of deuterium shows a shift in

the distribution of peaks due to the addition of the heavier isotope. This shift

corresponded to the amount of deuterium being acquired by the peptide. 20x GSNO was

used to ensure the availability of the substrate in the reaction to enable easy observation

of the interaction with the active site and the proposed allosteric site. Three of the four

amino acid residues that were implicated to be involved in the interaction at the proposed

site by computational studies are represented by the identified peptide list (appendix B).

They are Lys188, Lys323 and Gly321.The results from the two- and four- seconds

experiment showed that most of the peptides had an increase in the uptake of deuterium and is summarized in Table 1.5.1. All other relevant results are in appendix B.

Table 1.5.1 Change in Deuterium uptake by the residues implicated in allosteric binding.

	2 sec Exchange Δ Deuterium Uptake (%)	4 sec Exchange Δ Deuterium Uptake (%)	Representing Peptide Sequence
Asn185	N/A	N/A	N/A
Gly321	-0.9	+0.1	(W)/KGTAFGGWKS(V)
	-1.4	+0.5	(F)/GGWKSVESVPK(L)
Lys188	-0.4	-0.6	(T)AKLEPGSVC(A)
Lys323	-1.4	+0.5	(F)/GGWKSVESVPK(L)

The Gly321, Lys188 and Lys323 residues that are associated with the allosteric site were identified by peptide MS-MS. These residues as well as those that surround the GSNO molecule from the computational study all showed a decrease in the uptake of deuterium. Lys323 showed the highest rate of decrease at 1.4%, Lys188 a decrease of 0.4% and Gly321 which was represented twice on the peptide list showed decreases of 0.9% and 1.4%. Peptides leading to the active site pocket as well as those involved in the binding of NADH and the catalytic zinc also showed a decrease in the uptake of deuterium. The 2 second exchange provided changes in peptide within the ranges of -

1.8% to + 3.4% and -5.2% to +5.1% for deuterium uptake, respectively. These results

support the presence of the allosteric site on the enzyme GSNOR as proposed.

1.6 Method and Materials

1.6.1 GSNOR WT cloning and Protein isolation

The ADH5 cDNA used for this project was initially cloned by Dr. Bei Sun, who also

performed mutagenesis on said gene that resulted in the recombinant GSNOR with 6x-

histidine tags at each terminus as outline in appendix A. The pET28b_ADH5 was then

transformed into BL21(DE3) E.coli cells to facilitate purification of the enzyme.

   Protein purification begins with a single colony from the transformed BL21 cells

grown on LB Kanamycin agar plates. The colony is grown in a sterile polypropylene

culture tube containing 4ml of 2x YT media with 50 µg/ml of Kanamycin. The culture

tubes are left to grow overnight at 37ºC while shaking for further use in growing a starter

culture at a rate of 1ml of colony per 100ml of media under the same conditions. The

starter culture is used to inoculate 1.5L of 2x YT media containing 50 µg/ml of

Kanamycin and grown at 37 ºC until an optical density of 0.5-0.6 is reached. At this

point, GSNOR expression is induced by the addition of IPTG to a final concentration of

0.4mM. The induced culture was left for 24 hours at room temperature with shaking to

incubate. The cells were then collected by centrifugation at 6000rpm, 4ºC for 30 minutes.

The supernatant was discarded, and the pellet resuspended with lysis buffer, composed of

50mM Tris-HCl, 150mM NaCl, 15mM imidazole, 1mM DTT, 1mM PMSF, 1% Triton

X-100, 75µg/ml DNase I and 100µg/ml Lysozyme at pH8. The lysate was incubated on

ice for 30mins and further lysed by pulse sonification (20 seconds on and 20 seconds off

for a total of 8 pulses). Another round of centrifugation at 12000rpm,4ºC for 30mins was

performed and the supernatant further purified using a HIS-select Nickel Affinity Gel from Sigma-Aldrich (P6611).

The Nickel column was equilibrated with a wash buffer (with no imidazole) and Affinity purification was performed by following the manufacturer's protocol published by Sigma with modifications to buffer compositions. The wash buffer was composed of 50mM Tris-HCl, 150mM NaCl and 40mM imidazole, while the elution buffer was composed of 50mM Tris-HCl, 150mM NaCl and 300mM imidazole both at pH 8. The eluted protein was then buffer exchanged into a storage solution at pH 7.4, composed of 58mM Na_2HPO_4, 17mM of $na_2H_2PO_4$, 68mM NaCl and 15% glycerol, using Amicon centrifugal 30,000 NMWL filter (Millipore sigma UFC 903008) and stored at -80ºC.

1.6.2 GSNO synthesis

Reduced glutathione was dissolved in a solution of cold water and 2 M HCl. An equal amount of sodium nitrite was added, and the reaction mixture was stirred at 4ºC in the dark for 40 minutes. GSNO was then precipitated using 10 mL of cold acetone and the final pink product was washed with cold water and cold acetone before it was lyophilized for storage at -20ºC. All steps followed as per Hart's method.[80] The final product was verified by obtaining absorbance readings at 335 nm.

1.6.3 GSNOR Kinetics

Steady state analysis was performed on GSNOR WT and three mutants by varying GSNO as the substrate while keeping enzyme and NADH constant. A stock solution of 20mM NADH was prepared using milli-Q water. GSNO stock solutions of 1mM and 10mM were freshly prepared for each experiment using PBS buffer. GSNO of increasing concentration was added to a cuvette containing $80\mu M$ of NADH and PBS to a final reaction volume of $500\mu l$. The reaction was initiated by the addition of $2\mu g$ of enzyme. The consumption of NADH during the reaction was monitored using the decrease in absorbance at 340nm over a period of 60 seconds using the Agilent 8453 UV/Vis spectrophotometer. The rate of the initial linear decrease corresponding to NADH uptake was plotted in correlation to the concentration of GSNO. From this, K_M, V_{max} and Catalytic efficiency k_{cat} were calculated.

1.7 Results

Steady state analysis of GSNOR WT revealed a sigmoidal deviation [Figure 1.7.1 (i)] resulting in positive cooperativity. This led to the proposal of a possible allosteric site on the enzyme. Molecular docking simulations were performed to further investigate the presence of the allosteric binding site for the substrate GSNO. Hydrogen-Deuterium exchange experiments were also performed by Kathleen Fontana to investigate direct ligand interactions as per appendix B.

1.7.1 GSNOR Kinetics

Steady state kinetic assays of the WT were performed with the concentrations of NADH and enzyme kept constant while the concentration of GSNO was varied from 0uM to 700uM. Upon analysis of experimental data obtained, the apparent K_M, and V_{max} were calculated and are summarized in Table 1.5.1. The Hill coefficient was used to quantitatively determine the cooperativity of ligand binding. The Hill constant observed was 1.61 ± 0.14. Mutations at the proposed allosteric binding site were used to observe changes in the rate of ligand binding and how important the Lysine residues are for binding. Lysine (K) residues at position 188 and 323 were mutated to alanine (A). Three mutants were studied; a double mutant and single mutants at each position. For each mutant K_M, V_{max} were determined. Hill constant (n) obtained from the data set are summarized in table 1.5.1. From the Hill constant obtained, it was inferred that the

enzyme was displayed positive cooperativity for the WT while the mutant K188A loses the sigmoidal activity. Negative cooperativity can be seen for the mutants K323A and K188/323A. This shows that both WT and K188A have an affinity for the ligand to bind at this site however once the mutation at the other position as well as the double mutation occurs all ligand binding affinity was lost.

Table 1.7.1: Summary of experimental data obtained for the KM, Vmax, Hill constant, Kcat and the catalytic efficiency of GSNOR WT and three mutants

	WT	K188A	K323A	K188/323A
K_M (µM)	22.01 ± 3.8	28.51 ± 4.7	N/D	N/D
V_{max} (µM/s)	0.0058 ± 0.0003	0.0052 ± 0.0003	0.0012 ± 0.0003	0.0019 ± 0.0001
Hill constant (n)	1.61 ± 0.14	0.9 ± 0.085	0.1 ± 0.014	0.34 ± 0.21
K_{cat} (s^{-1})	58,000	52,000	12,000	19,000
K_{cat}/K_M ($s^{-1}µM^{-1}$)	2,624	1,824	N/D	N/D
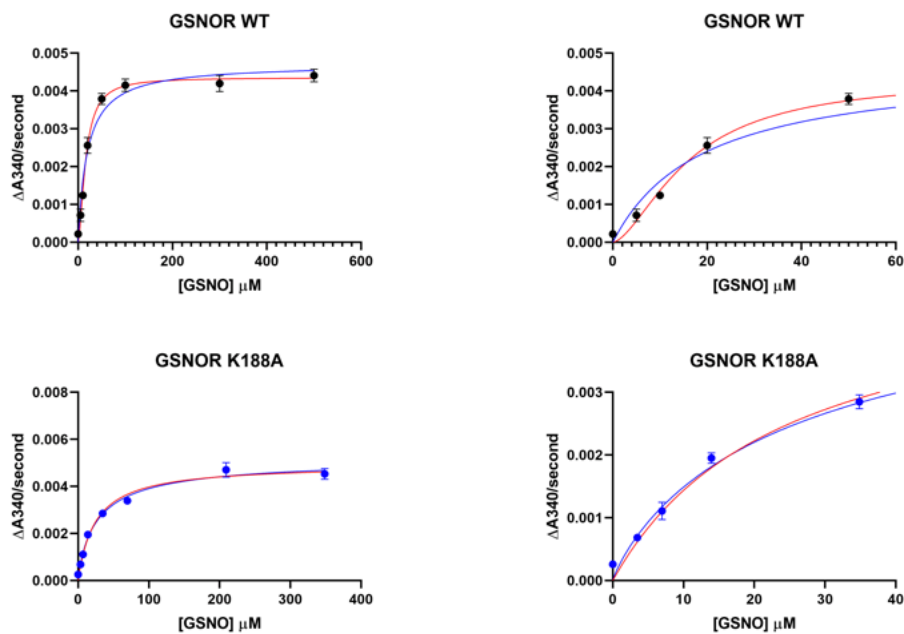
Figure 1.7.1 (i) Plots of the kinetic data obtained for GSNOR WT and GSNOR K188A. The left panel shows the full Michaelis Menten plots (blue line) as well as the sigmoidal curve (red line) however the deviation cannot be seen. The right panel shows a zoom in plot at the lower concentrations, this shows the deviations from the classical Michaelis Menten plot.
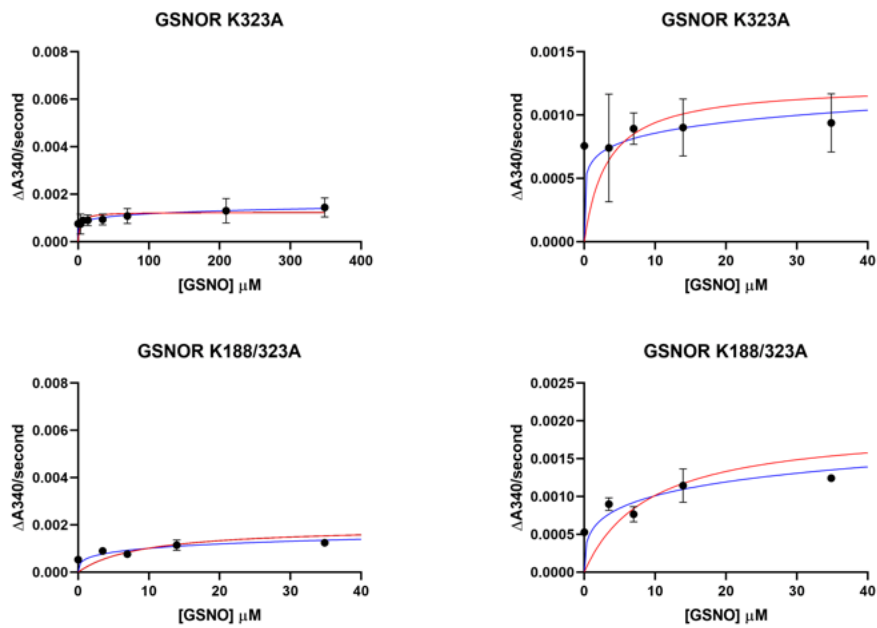
Figure 1.7.1.ii Plots of the kinetic data obtained for GSNOR K323A and GSNOR K188/323A. The left panel shows the full Michaelis Menten plots (blue line) as well as the sigmoidal curve (red line) however the deviation cannot be seen. The right panel shows a zoom in plot at the lower concentrations, this shows the deviations from the classical Michaelis Menten plot.

27

1.8 Discussion

The data obtained from the computational, steady state kinetics and HDX-MS studies of GSNOR support the hypothesis that there is indeed an allosteric site for the binding of the substrate GSNO present on the enzyme GSNOR.

The steady state assay first performed on GSNOR WT showed a slight deviation from the Michalis Menten plot when a Hill constant was applied to fit a sigmoidal curve which led to the hypothesis of the presence of the proposed allosteric site and the desire to study it. In an attempt to understand how the presence of an allosteric site affects enzyme function, mutational study was done.

The steady state assay performed gave results that show difference in K_M, V_{max}, and Hill constant. As table 1.5.1 shows the WT and mutant K188A show K_M values that are close to the literature value of $27 \mu M$[81] while the K_M values of K323A and K188/323A decreases drastically. This shows that the mutations occurring at these sites lead to an almost complete loss in affinity for substrate binding that could be because of conformational changes in the enzyme structure. This was further confirmed by the Hill constant which showed positive cooperativity for the WT, non-cooperativity for the mutant K188A and negative cooperativity for the other mutants. The graphs show a slow rate moving towards the K_M but a much faster rate on its way to the V_{max}. The steady state data shows that although the computational study suggests that Lys323 does not interact directly with the substrate, the almost complete loss of activity after mutation suggests otherwise.

28

These results show that the activity of GSNOR is hyper-sensitive to structural changes at this other-than the active site. This is favorable for pharmaceutical companies that have been investigating the inhibition of this enzyme for treating diseases affiliated with the enzyme. This discovery could aid the company in designing small molecules that can attack the lysine residue at position 323 for instance.

1.9 Conclusion

The results obtained from (1) the steady state assay with a Hill constant of 1.61±0.14 for GSNOR WT and decreasing Hill constant for the mutants; (2) the results from the HDX-MS which showed a decrease in deuterium uptake of 1.4%, 0.4%, 0.9% and 1.4% for Lys323, Lys188, and (3) the two Gly321 peptides identified from the reaction of GSNOR and excess GSNO reaction; support the hypothesis that the enzyme GSNOR has an allosteric site present that binds the substrate GSNO, increases its rate of reaction, and is more fitted to the sigmoidal curve plot than the classical Michalis Menten. This site could be a potential target for pharmaceutical company in developing molecules that can disrupt GSNOR's activity by attacking there.

1.10 Future direction

    To confirm the location and presence of an allosteric site, several steps may be taken in future experiments. First the mutation of the Lysine residue to another residue similar in size and charge to determine if the loss of the charge or the bulk side chain plays a role in the loss of affinity for the substrate. In addition, more HDX-MS trials should be performed to provide further confirmation.

CHAPTER 2

Development of fluorogenic pseudo-substrates

Chapter Summary

      This chapter describes the theoretical basis and the methods employed in synthesizing and characterizing four fluorogenic probes/pseudo substrates. The four probes synthesized are *N,N*-di(thioamido-fluoresceinyl)-cystine (DTFCys$_2$), *N,N*-di(thioamido-fluoresceinyl)-homocystine (DTFHCys$_2$), *N*-amido-*O*-aminobenzoyl-*S*-nitrosoglutathione (AOASNOG), and *N*-thioamido-fluoresceinyl-*S*-nitroso-glutathione (TFSNOG). These probes can be used in measuring and imaging free thiols present on cell surfaces, as substrates for the thiol reductase and S-nitrosothiol denitrosylase activities of the protein disulfide isomerase (PDI). It can also be used as a substrate for the S-nitrosothiol reductase activity of GSNOR in vitro and on live cells.

2.1 Fluorescence: A brief introduction

Fluorescence is a luminescence process involving susceptible molecules that emit light from electronically excited states made by either a physical or chemical mechanism. Fluorescence occurs by the absorption of photons in a singlet ground state to a singlet excited state. As the excited molecule returns to the ground state, it emits a photon of lower energy that corresponds to a longer wavelength than the absorbed photon. The energy loss is due to vibrational relaxation while in the excited state. Fluorescent bands center at wavelengths longer this shift towards the longer wavelengths is known as the stokes shift.[82] Excited states are short-lived with a lifetime at about 10^{-8} seconds. Substance luminescence is affected by the molecular structure and the chemical environment. The molecular structure and chemical environment also determine the intensity of emission when luminescence does occur. In general molecules that can fluoresce are conjugated systems and the specific frequencies of excitation and emission are dependent on the molecule or atom.
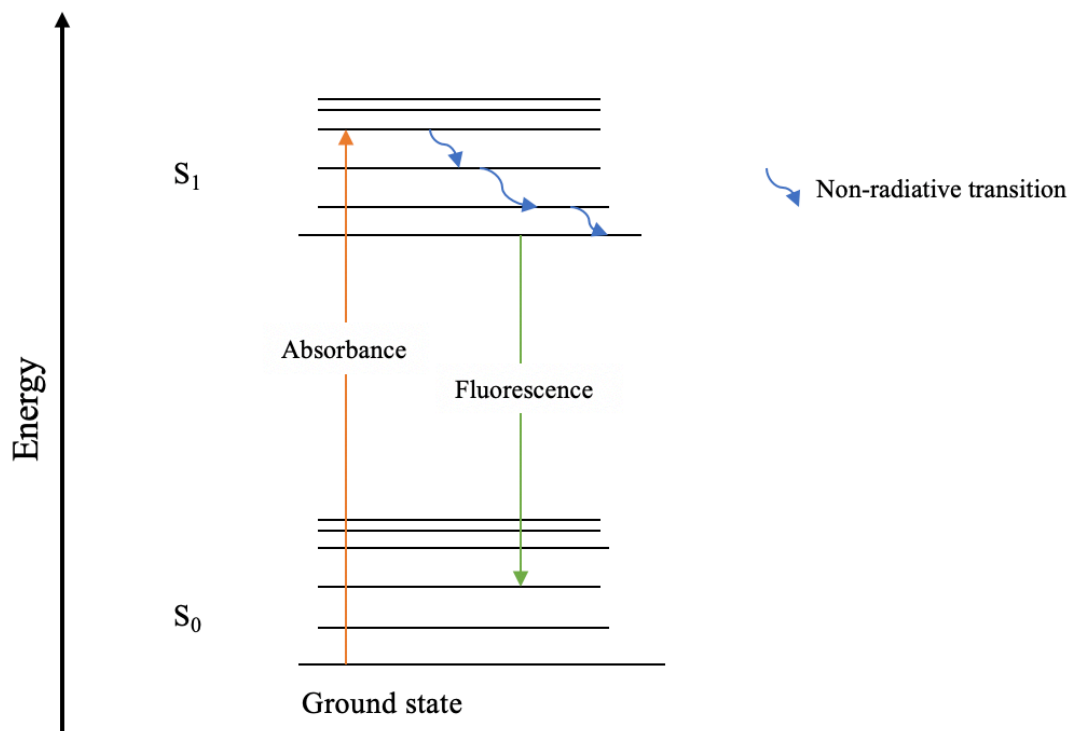
Figure 2.1 Jablonski diagram of absorbance, non-radiative decay and fluorescence.

2.2 Fluorescein

The fluorescein dye is the most commonly used fluorescent probe due to its high molar absorptivity at a wavelength 494nm, making it a very useful and sensitive fluorescent label. Fluorescein is commercially available in many derivatives, the major one been Fluorescein isothiocyanate. Fluorescein isothiocyanate (FITC) is simply the original fluorescein molecule that was functionalized with an isothiocyanate reactive group which replace a hydrogen atom on the bottom ring of the structure. FITC is often used in cellular biology to label and track cells in fluorescence microscopy applications. FITC reacts readily with nucleophiles such as the amine and sulfhydryl groups of proteins. Many moieties can be conjugated with FITC making them useful in a wide variety of experimental procedures from immunofluorescence, Apoptosis detection, Nucleotide labelling, to in situ hybridization and many more.[83]
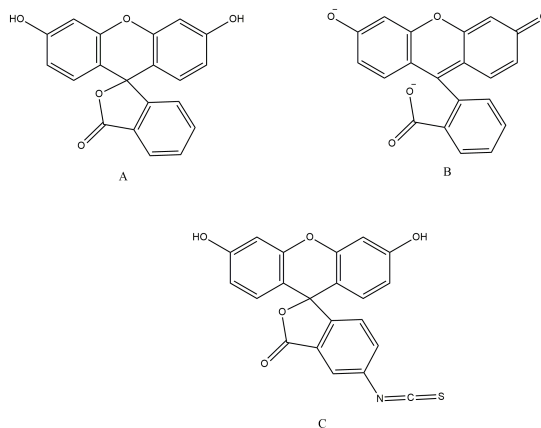
Figure 2.2 A shows the fluorescein molecule, B shows the dianion form of fluorescein which give the best intensity of fluorescence and C shows the functionalized fluorescein molecule, the Fluorescein isothiocyanate derivative

2.3 The redox probes

The highlighted reagents would theoretically act as probes and pseudo substrates for several reactions. Three of such reactions are the enzyme catalyzed disulfide reduction (Equation 2.3.1), S-nitrosothiol denitrosylation by the release of NO or HNO (Equation 2.3.2) and the reduction of NO^+ to NH_2OH (Equation 2.3.3).

$$R\text{-}S\text{-}S\text{-}R \longrightarrow 2\ RSH \qquad\qquad \text{Equation 2.3.1}$$

$$R\text{-}S\text{-}N{=}O \longrightarrow NO + \tfrac{1}{2}\ RS\text{-}SR \qquad\qquad \text{Equation 2.3.2}$$

$$R\text{-}S\text{-}N{=}O \longrightarrow NH2OH + \tfrac{1}{2}\ RS\text{-}SR \qquad\qquad \text{Equation 2.3.3}$$
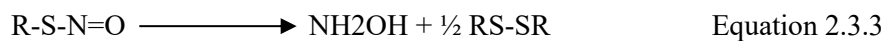
The four probes are fluorogenic, therefore when they partake in thiol redox reactions an increase in their fluorescence can be observed. The probes are *N,N*-di(thioamido-fluoresceinyl)-cystine (DTFCys$_2$, figure 2.3A), *N,N*-di(thioamido-fluoresceinyl)-homocystine (DTFHCys$_2$, figure 2.3B), *N*-amido-*O*-aminobenzoyl-*S*-nitrosoglutathione (AOASNOG, figure 2.3D), and *N*-thioamido-fluoresceinyl-*S*-nitroso-glutathione (TFSNOG, figure 2.3C). Intra-molecular quenching in these probes account for their low fluorescence when they are not a part of a reaction. Quenching in DTFCys2 is due to the proximity of the two fluorophores to each as a result of structural stability via intramolecular H-bonding. The self-quenching is results from the collisional energy transfer that leads to thermalization of the electronic excitation energy. Fluorescence quenching in AOASNOG and TFSNOG occurs due to the overlap in spectrum of the functional group, S-N=O (λ_{max} = 312nm and 545nm) with either the excitation (λ_{max} =

494nm) or emission (λ_{max} = 520nm) spectrum of fluorescein because of the close

proximity of the functional group to the fluorophore.
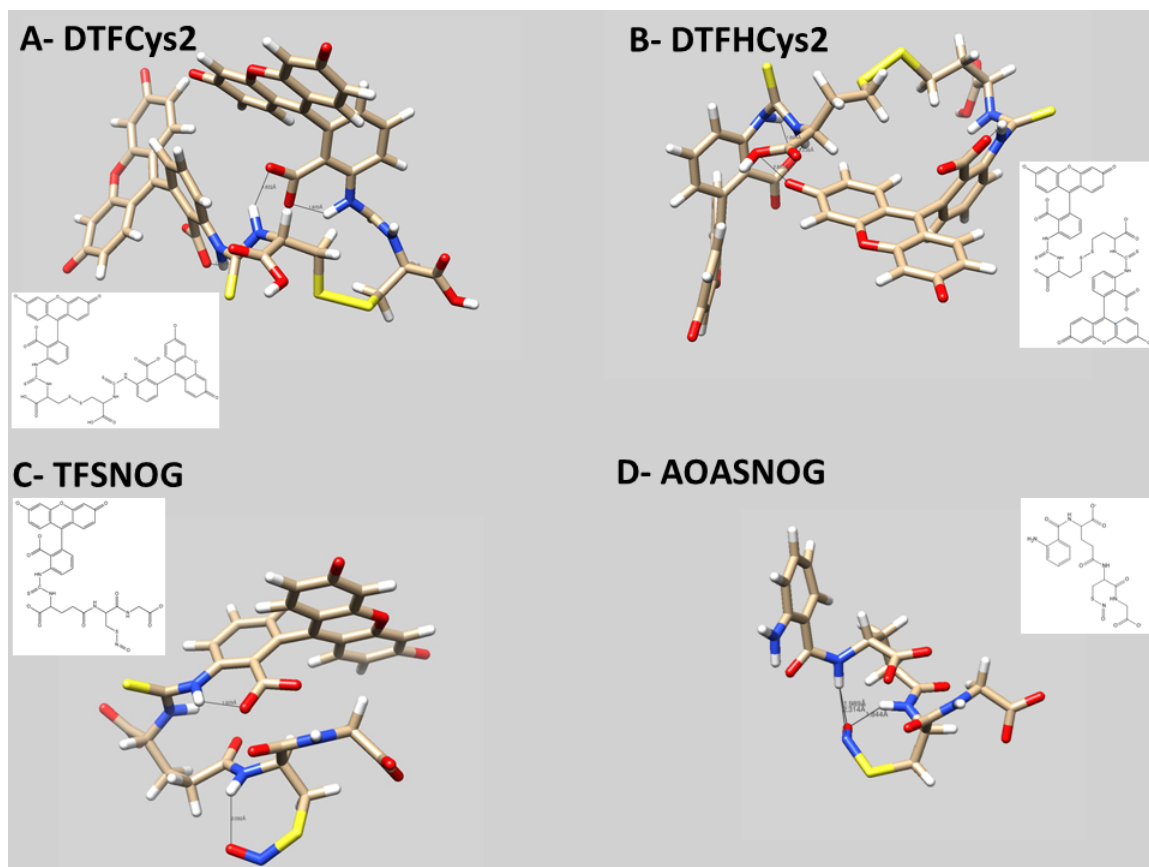
Figure 2.3 MM2 energy minimized and 2D structures of A- DTFCys2, B- DTFHCys2, C-TFSNOG and D-AOASNOG. The black lines indicate intramolecular H-bonds

2.4 Materials

Glutathione (reduced), Isatoic anhydride, fluorescein isothiocyanate (FITC), Cystine, Homocystine, and sephadex G-50 were all purchased from Sigma Aldrich. Silica plate[TM] TLC plates were purchased from SiliCycle Inc.

2.5 Methods

2.5.1 *N,N*-di(thioamido-fluoresceinyl)-cystine (DTFCys$_2$, figure 2.3.1A)

L-Cystine (0.1mmol) was dissolved in 3.0mL of 0.1M sodium carbonate solution. This was added to a solution of 0.25mmol FITC dissolved in 3.0mL of acetone. This was left to react for 24 hours at 50°C protected from light. The reaction mixture was lyophilized and applied onto a 2.5cm x 30cm Econo column filled with Sephadex G-50 that has been equilibrated with water. DTFCys$_2$ was eluted using 3 column volumes and the fraction was concentrated by lyophilization, dissolved in water and divided into 100mL aliquots for freezing at -20°C. The final product was characterized using NMR, UV/Vis, and Fluorescence spectroscopy. The ^{1}H-NMR spectrum was characterized by the fluoresceinyl-protons ranging from 5.7 to 7.4ppm, and multiplets corresponding to the Cys protons all summarized in Table C1 of appendix C. The UV/Vis spectrum was characterized by the large fluoresceinyl-absorbance peak (λ_{max} = 494nm, ε_M=176,000 M^{-1}cm^{-1}). There was also a shoulder due to the fluoresceinyl-moieties overlapping at 475nm. The absorbance contributions of the S-N=O moiety was buried within the broad aromatic contribution from the fluorescein moiety.

2.5.2 *N,N*-di(thioamido-fluoresceinyl)-homocystine (DTFHCys$_2$, figure 2.3.2B)

The procedure for the synthesis of DTFHCys$_2$ was the same as that used for

DTFCys$_2$ with 0.1mmol L-Homocystine. The final product was characterized using

NMR, UV/Vis, and Fluorescence spectroscopy. The ^{1}H-NMR spectrum was like that of

DTCys$_2$ with the addition of two peaks all summarized in Table C1 of appendix C. The

UV/Vis spectrum was characterized by the large fluoresceinyl-absorbance peak (λ_{max} =

494nm, ε_M=176,000 M^{-1}cm^{-1}). There was also a shoulder due to the fluoresceinyl-

moieties overlapping at 475nm that was seen for DTFCys$_2$.

2.5.3 *N*-amido-*O*-aminobenzoyl-*S*-nitrosoglutathione (AOASNOG, figure 2.3.2D)

S-nitrosoglutathione was synthesized using Hart's Method.80 SNOG (0.32mmol)

and 1.84mmol Isatoic anhydride (recrystallized from isopropanol) which were dissolved

in 0.5M phosphate buffer pH8 and left to react for 24 hours at 22°C protected from light.

The reaction mixture was applied to a 1cm x 10cm Econo column packed with 1g of

QAE-Sephadex equilibrated with water. The column was washed with 50mL of water

and the AOASNOG was eluted using 0.1M phosphate buffer containing 0.5M NaCl pH

7.4. The product was concentrated by lyophilization, dissolved in 2.0mL of water and

divided into aliquots for freezing at -20°C. AOASNOG was characterized using NMR,

UV/Vis, and Fluorescence spectroscopy. The 1H-NMR spectra of SNOG and

AOASNOG were compared. The largest chemical shift change observed in the

AOASNOG spectrum which indicated the presence of the o-aminobenzoyl group and

aromatic protons. The NMR results are summarized in Table C2 of appendix C.[84] The

UV/Vis spectrum is characterized by a broad peak that consist of the absorbance of

o-aminobenzoyl (λ_{max} = 312 nm, ε_M= 2,800 $M^{-1}cm^{-1}$) and a shoulder from the -SNO

group (λ_{max} = 335 nm, ε_M= 920 $M^{-1}cm^{-1}$). There was also a small contribution in the red

range (λ_{max} = 545 nm, ε_M=16 $M^{-1}cm^{-1}$) due to the second weaker -SNO absorbance.[85]

The fluorescence properties of AOASNOG have previously been detailed, further

confirming that AOASNOG is weakly fluorescent because of the close spatial and

overlapping spectra of the excitation spectrum of o-aminobenzoyl-moiety and the

-S-N=O absorbance. This shows that AOASNOG has the ability to act as a fluorogenic

reporter of chemical changes to the -S-N=O functionality through the loss of NO+ or the

reduction of -S-N=O to -S-NHOH by enzymes like S-nitrosoglutathione reductase

(GSNOR) leading to a 14 fold increase in fluorescence at 412nm.[84]

2.5.4 *N*-thioamido-fluoresceinyl-*S*-nitroso-glutathione (TFSNOG, figure 2.3.2C)

S-nitrosoglutathione (0.3mmol) was dissolved in 4mL of 0.2M $NaHCO_3$ pH 9. This

solution was then added to a solution of 0.1mmol FITC dissolved in 4mL of acetone.

This was left to react for 4 hours at 22°C protected from light. The product was applied to

a 1.5cm x 10cm Econo column packed with 2mL of Dowex-1 (Cl⁻ form). FITC and GSH

do not have a strong interaction with the Dowex-1 because at pH 7 they have net charges

of -2 and -1, respectively. However, TFSNOG at pH 7 has a net charge of -4 and has a strong interaction with the Dowex-1. Isolation of the product was started by washing the with 50mL of 0.1M Tris-HCl pH 7.4 and the TFSNOG eluted using the same buffer containing 1M NaCl. The eluate was concentrated by lyophilization then re-dissolved in 0.5mL of water and desalted on a packed column of 15mL Sephadex G-25 equilibrated using distilled water. The fraction containing TFSNOG was collected, concentrated by lyophilization, and divided into aliquots for freezing at -20°C.

TFSNOG was characterized using NMR, UV/Vis, and Fluorescence spectroscopy. The 1H-NMR spectra of TFSNOG showed a range of 6.3ppm to 7.6ppm for the aromatic protons of the fluoresceinyl-moiety and peaks for multiplets corresponding to the proton of Glu and Gly of SNOG all summarized in Table C1 of appendix C. UV/Vis spectrum of TFSNOG showed a large absorbance peak for the fluoresceinyl-moiety (λ_{max} = 494 nm, ε_M=88,000 $M^{-1}cm^{-1}$) with the contribution from the -SNO moiety buried within the broad peak. TFSNOG has a low fluorescence because of the overlap between the -S-N=O absorbance, λ_{max} = 545nm and the fluoresceinyl-emission, λ_{max} = 520 nm. The fluorescence increases upon denitrosylation with DTT.

2.6 Results
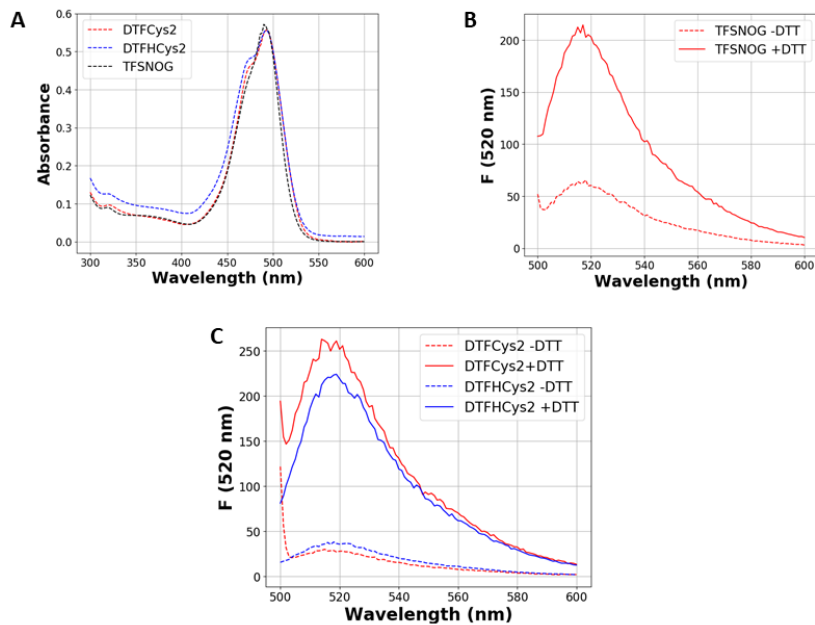
Figure 2.6 A: UV/Vis spectrum of DTFCys₂ (red dash line), DTFHCys₂ (blue dash line) and TFSNOG (black dash line); B: Fluorescence emission spectrum of TFSNOG before (dash line) and after the addition of DTT (50μM, red line); C: Fluorescence emission spectrum of DTFCys₂ before (red dash) and after the addition of DTT (50μM, red line). Fluorescence emission spectrum of DTFHCys₂ before (blue dash) and after the addition of DTT (50μM, blue line).

2.6.1 Free thiol determination

DTFCys$_2$ and DTFHCys$_2$ can be used as fluorescent reagents for detecting free thiol concentration just like Ellman's reagent[86] via the thiol disulfide exchange shown in Equation 2.6.1. This reagent can be used to determine nmol levels of free thiols (Figure 2.6.1).

$$\text{F-Cys-S-S-Cys-F} + \text{RS}^- \rightarrow \text{R-S-S-Cys-F} + \text{F-Cys-S}^- \qquad \textit{Equation 2.6.1}$$

low fluorescence   *higher fluorescence*

Figure 2.6.1 Constant volume of DTFCys$_2$ (A) and DTFHCys$_2$ (B) were added to the first 9 wells of a 96-well plate. The first two well were used as control and to wells 4-6 increasing amounts of DTT (blue) were added. Wells 7-9 had increasing amounts of GSH (red). Each point accounts for the increase in thiol concentration.

2.6.2 Kinetic Characterization of disulfide reductases in vitro and in live cells

Researchers had shown that cells have a cell surface associated form of PDI.[87-97] DTFCys2 can also be used to kinetically characterize pure recombinant PDI and cell surface PDI of ARPE cells. These reagents can also be used in imaging cell surface thiols from PDI to other free protein thiols on live cells. Figure 2.6.2b shows ARPE cells exposed to DTFCys$_2$.
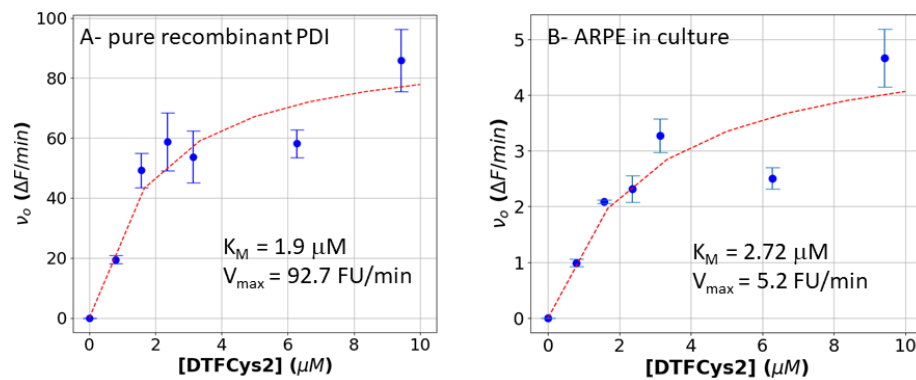
Figure 2.6.2a; A: constant volume of purified recombinant PDI was added to 96-well plates with increasing amounts of DTFCys$_2$ and enzymatic reaction was initiated by the addition of DTT. B: ARPE cells grown to confluence in wells of a 96-well plate had increasing amounts of DTFCys$_2$ added to it the wells and change in fluorescence was monitored at 520nm for 9 minutes. The fit used to estimate the value of KM is showed as the red dashed line.
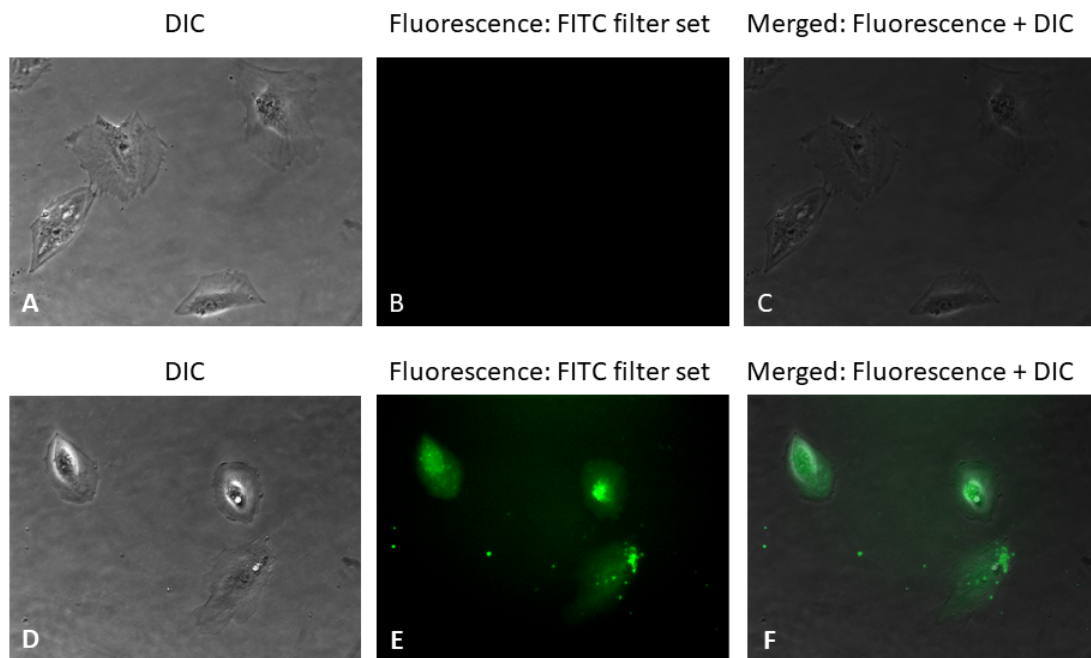
Figure 2.6.2b ARPE cells grown at the bottom of 96-well plates exposed to PBS (control)- panel A, B, C and DTFCys2- Panel D, E, F for 15 mins. imaged from the bottom of the plate using an inverted epifluorescence microscope (Zeiss Axiovert 200) equipped with an FITC cube. Overlay of the DIC images of the cells done with the aid of Corel paint shop pro 2018.

2.6.3 Kinetic characterization of S-nitrosoglutathione reductase in vitro and live cells

AOASNOG is currently the only cell permeable, pseudo-substrate for S-nitrosoglutathione reductase.[84] This section demonstrates how it can be used to kinetically characterize ARPE cells (Figure 2.6.3B). TFSNOG the fluorescein analog of AOASNOG acts as a pseudo-substrate for the S-denitrosylation activity of PDI.[98]
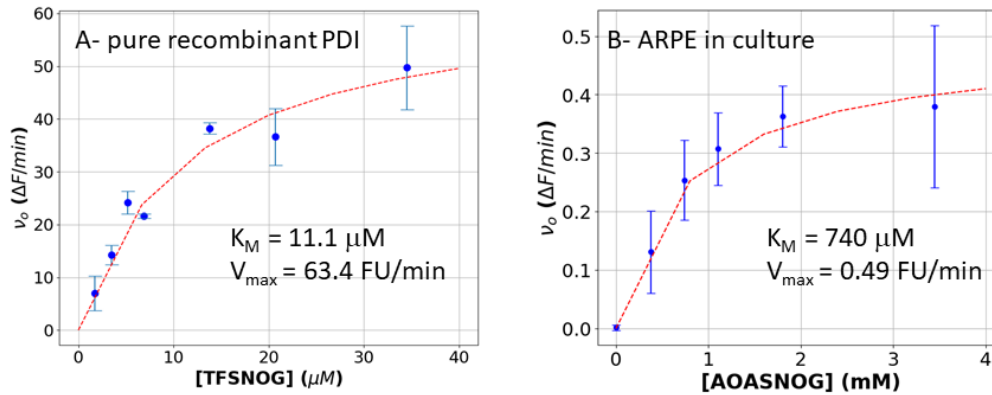
Figure 2.6.3 A: constant volume of purified PDI with increasing amounts of TFSNOG were added to the wells of a 96-well plate and enzymatic activity was initiated by the addition of DTT. B: ARPE cells grown to confluence in wells of a clear 96-well plate had increasing amounts of AOASNOG added to the wells. Changes in fluorescence was monitored at 520nm (A) and 412 (B) every 35s for 9 minutes.

2.7 Discussion

The purpose of this study was to describe the theoretical basis and simple methods for synthesizing four probes/reagents that can be used in various applications such as the measuring and imaging of free thiols on cell surface as well as how they can perform as pseudo-substrates for monitoring enzymatic activities. Each reagent was characterized using NMR as well as UV/Vis and Fluorescence spectroscopy. Thin Layer Chromatography (TLC) was performed using SiliaPlate TLC aluminum backed plates with varying mobile phases that provided the best separation. The mobile phase used for DTFCys2, DTFHCys2, and TFSNOG was acetone:water:methanol in a 10:10:1 ratio. For AOASNOG the mobile phase composition was acetone:water:methanol in a 13:6:1 ratio. The multiple spots observed for FITC are due to the different prototrophic forms of fluorescein.[107]

The disulfide-linked probes DTFCys2 and DTFHCys2 can function as fluorescent reagents for the detection of free thiol concentrations just like the classical colorimetric thiol reagent 5,5'-dithiobis-2-nitrobenzoate (Ellman's reagent) from the thiol disulfide exchange. However, unlike the Ellman's reagent, the fluorescence signal from these new regents enables the detection of thiol concentrations in the nmol levels. DTFCys2 can be used to kinetically characterize recombinant PDI and cell surface PDI of ARPE in culture with estimated K_M for the PDI mediated disulfide reduction which was ~1.9μM and was close to the estimated K_M for the ARPE-surface PDI of 2.72μM. the Michaelis Menten equation was used to estimate the steady-state kinetic parameters from a fit of the data. A

K_M of 740μM was estimated for AOASNOG in the ARPE-GSNOR catalyzed

denitrosation which comes close to the K_M for recombinant GSNOR of 320μM. TFSNOG

functions as a pseudo-substrate for the S-denitrosylase activity of PDI with an estimated

K_M of 11.1μM that corresponds to a higher affinity of about 6-fold compared to that of

SNOG (65μM). Unfortunately, TFSNOG was not a pseudo-substrate for GSNOR. Apart

from the large applications to enzymology and cell biology, the reagents cost less to

produce because the fluorescein isothiocyanate is less expensive than eosin

isothiocyanate for example. In addition, fluorescein derivatives are much easier to purify.

2.8 Conclusion

The reagents outlined here are easy to prepare and purify. They can be used in

diverse applications ranging from their use as thiol reagents to pseudo-substrates for

monitoring enzymatic activities in vitro.

REFERENCES/BIBLIOGRAPHY

1. Furchgott, R. F.; Zawadski, J. Acetylcholine Relaxes Arterial Smooth-Muscle by Releasing a Relaxing Substance from Endothelial-Cells. *Fed Proc* **39:**581-581; 1980.

2. Ignarro, L. J.; Buga, G. M.; Wood, K. S.; Byrns, R. E.; Chaudhuri, G. Endothelium-Derived Relaxing Factor Produced and Released from Artery and Vein Is Nitric-Oxide. *P Natl Acad Sci USA* **84:**9265-9269; 1987.

3. Palmer, R. M. J.; Ferrige, A. G.; Moncada, S. Nitric-Oxide Release Accounts for the Biological-Activity of Endothelium-Derived Relaxing Factor. *Nature* **327:**524-526; 1987.

4. Furchgott, R. F.; Khan, M. T.; Jothianandan, D. Comparison of Endothelium-Dependent Relaxation and Nitric Oxide-Induced Relaxation in Rabbit Aorta. *Fed Proc* **46:**385-385; 1987.

5. Sun, B. Biochemical and Functional Studies of S-nitrosoglutathione Reductase and Neutral Sphingomyelinase II. University of Windsor, Electronic Theses and Dissertations, 2017

6. Moncada, S.; Radomski, M. W.; Palmer, R. M. J. Endothelium-Derived Relaxing Factor - Identification as Nitric-Oxide and Role in the Control of Vascular Tone and Platelet-Function. *Biochem Pharmacol* **37:**2495-2501; 1988.

7. Ignarro, L. J.; Byrns, R. E.; Burga, G. M.; Wood, K. S., Endothelium-Derived Relaxing Factor From Pulmonary Artery and Vein Possesses Pharmacologic and

Chemical Properties Identical to Those of Nitric Oxide Radical. *Circulation Research* **1987,** *61* (6), 866-879.

8. Ignarro, L. J.; Burga, G. M.; Wood, K. S.; Byrns, R. E.; Chaudhuri, G., Endothelium-derived relaxing factor produced and released from artery and vein is nitric oxide. *Proc Natl Acad Sci U S A* **1987,** *84* (24), 9265-9269

9. Stuehr, D. J.; Kwon, N. S.; Nathan, C. F.; Griffith, O. W.; Feldman, P. L.; Wiseman, J. N omega-hydroxy-L-arginine is an intermediate in the biosynthesis of nitric oxide from L-arginine. *J Biol Chem* **266:**6259-6263; 1991.

10. Knowles, R. G.; Moncada, S. Nitric-Oxide Synthases in Mammals. *Biochem J* **298:**249-258; 1994.

11. Forstermann, U.; Closs, E. I.; Pollock, J. S.; Nakane, M.; Schwarz, P.; Gath, I.; Kleinert, H. Nitric-Oxide Synthase Isozymes - Characterization, Purification, Molecular- Cloning, and Functions. *Hypertension* **23:**1121-1131; 1994.

12. Forstermann, U.; Sessa, W. C. Nitric oxide synthases: regulation and function. *Eur Heart J* **33:**829-+; 2012.

13. Bohme, G. A.; Bon, C.; Lemaire, M.; Reibaud, M.; Piot, O.; Stutzmann, J. M.; Doble, A.; Blanchard, J. C. Altered Synaptic Plasticity and Memory Formation in Nitric- Oxide Synthase Inhibitor-Treated Rats. *P Natl Acad Sci USA* **90:**9191-9194; 1993.

14. Zhou, L.; Zhu, D. Y. Neuronal nitric oxide synthase: Structure, subcellular localization, regulation, and clinical implications. *Nitric Oxide-Biol Ch* **20:**223-230;

2009.

15. Togashi, H.; Sakuma, I.; Yoshioka, M.; Kobayashi, T.; Yasuda, H.; Kitabatake, A.; Saito, H.; Gross, S. S.; Levi, R. A Central-Nervous-System Action of Nitric-Oxide in Blood-Pressure Regulation. *J Pharmacol Exp Ther* **262:**343-347; 1992.

16. Esplugues, J. V. NO as a signalling molecule in the nervous system. *Brit J Pharmacol* **135:**1079-1095; 2002.

17. Kolios, G.; Valatas, V.; Ward, S. G., Nitric oxide in inflammatory bowel disease: a universal messenger in an unsolved puzzle. *Immunology* **2004,** *113* (4), 427-437.

18. Nathan, C. F.; Hibbs, J. B. Role of Nitric-Oxide Synthesis in Macrophage Antimicrobial Activity. *Current Opinion in Immunology* **3:**65-70; 1991.

19. Fleming, I.; Busse, R. Molecular mechanisms involved in the regulation of the endothelial nitric oxide synthase. *Am J Physiol-Reg I* **284:**R1-R12; 2003.

20. Azuma, H.; Ishikawa, M.; Sekizaki, S. Endothelium-Dependent Inhibition of Platelet-Aggregation. *Brit J Pharmacol* **88:**411-415; 1986.

21. Li, H. G.; Forstermann, U. Nitric oxide in the pathogenesis of vascular disease. *Journal of Pathology* **190:**244-254; 2000.

22. Martínez-Ruiz, A., Cadenas, S., & Lamas, S. (2011). Nitric oxide signaling: Classical, less classical, and nonclassical mechanisms. *Free Radical Biology And Medicine*, *51*(1), 17-29. doi: 10.1016/j.freeradbiomed.2011.04.010

23. Brown, G. C.; Cooper, C. E. Nanomolar Concentrations of Nitric-Oxide Reversibly Inhibit Synaptosomal Respiration by Competing with Oxygen at Cytochrome-

Oxidase. *Febs Lett* **356:**295-298; 1994.

24. Martinez-Ruiz, A.; Cadenas, S.; Lamas, S. Nitric oxide signaling: Classical, less classical, and nonclassical mechanisms. *Free Radical Bio Med* **51:**17-29; 2011.

25. Erusalimsky, J. D.; Moncada, S. Nitric oxide and mitochondrial signaling from physiology to pathophysiology. *Arterioscl Throm Vas* **27:**2524-2531; 2007.

26. Hess, D., Matsumoto, A., Kim, S., Marshall, H., & Stamler, J. (2005). Protein S-nitrosylation: purview and parameters. *Nature Reviews Molecular Cell Biology*, *6*(2), 150-166. doi: 10.1038/nrm1569

27. Forman, H. J.; Fukuto, J. M.; Torres, M. Redox signaling: thiol chemistry defines which reactive oxygen and nitrogen species can act as second messengers. *Am J Physiol- Cell Ph* **287:**C246-C256; 2004.

28. Foster, M. W.; Hess, D. T.; Stamler, J. S. Protein S-nitrosylation in health and disease: a current perspective. *Trends Mol Med* **15:**391-404; 2009.

29. Hickok JR, Vasudevan D, Thatcher GRJ, and Thomas DD. Is S-nitrosocysteine a true surrogate for nitric oxide? Antioxid Redox Signal 17: 962–968, 2012.

30. Thomas, D. D. and D. Jourd'heuil (2012). "S-Nitrosation: Current Concepts and New Developments." <u>Antioxidants & Redox Signaling</u> **17**(7): 934-936.

31. Gow, A. J.; Buerk, D. G.; Ischiropoulos, H. A novel reaction mechanism for the formation of S-nitrosothiol in vivo. *J Biol Chem* **272:**2841-2845; 1997.

32. Benhar, M.; Forrester, M. T.; Stamler, J. S. Protein denitrosylation: enzymatic mechanisms and cellular functions. *Nat Rev Mol Cell Bio* **10:**721-732; 2009.

33. Benhar, M., Forrester, M., Hess, D., & Stamler, J. (2008). Regulated Protein Denitrosylation by Cytosolic and Mitochondrial Thioredoxins. *Science*, *320*(5879), 1050-1054. doi: 10.1126/science.1158265

34. Palmer, L., Kavoussi, P., & Lysiak, J. (2012). S-Nitrosylation of endothelial nitric oxide synthase alters erectile function. *Nitric Oxide*, *27*, S22-S23. doi: 10.1016/j.niox.2012.04.079

35. He, W., & Frost, M. (2016). Direct measurement of actual levels of nitric oxide (NO) in cell culture conditions using soluble NO donors. *Redox Biology*, *9*, 1-14. doi: 10.1016/j.redox.2016.05.002

36. Beuve, A., Wu, C., Cui, C., Liu, T., Jain, M., & Huang, C. et al. (2016). Identification of novel S-nitrosation sites in soluble guanylyl cyclase, the nitric oxide receptor. *Journal Of Proteomics*, *138*, 40-47. doi: 10.1016/j.jprot.2016.02.009

37. Guerra, D., Ballard, K., Truebridge, I., & Vierling, E. (2016). S-Nitrosation of Conserved Cysteines Modulates Activity and Stability of S-Nitrosoglutathione Reductase (GSNOR). *Biochemistry*, *55*(17), 2452-2464. doi: 10.1021/acs.biochem.5b01373

38. Jensen, D. E.; Belka, G. K.; Bois, G. C. D., S-Nitrosoglutathione is a substrate for rat alcohol dehydrogenase class III isoenzyme. *Biochem J* **1998,** *331*, 659-668.

39. Hedberg, J. J.; Hoog, J.-O.; Nilsson, J. A.; Xi, Z.; Elfwing, Å.; Grafstro, R. C., Expression of alcohol dehydrogenase 3 in tissue and cultured cells from human oral mucosa. *Am J Pathol* **2000,** *157* (5), 1745-1755.

40. Hopkinson, R. J.; Barlow, P. S.; Schofield, C. J.; Claridge, T. D. W., Studies on the reaction of glutathione and formaldehyde using NMR. *Org Biomol Chem* **2010,** *8* (24), 4915-4920.

41. Leterrier, M.; Chaki, M.; Airaki, M.; Valderrama, R.; Palma, J. M.; Barroso, J. B.; Corpas, F. J., Function of S-nitrosoglutathione reductase (GSNOR) in plant development and under biotic/abiotic stress. *Pant Signal Behav* **2011,** *6* (6), 789-793.

42. Fagerberg, L.; Hallstro, B. M.; Oksvold, P.; Kampf, C.; Djureinovic, D.; Odeberg, J.; Habuka, M.; Tahmasebpoor, S.; Danielsson, A.; Edlund, K.; Asplund, A.; Sjostedt, E.; Lundberg, E.; Szigyarto, C. A.-K.; Skogs, M.; Takanen, J. O.; Berling, H.; Tegel, H.; Mulder, J.; Nilsson, P.; Schwenk, J. M.; Lindskog, C.; Danielsson, F.; Mardinoglu, A.; Sivertsson, Å.; Feilitzen, K. v.; Forsberg, M.; Zwahlen, M.; Olsson, I.; Navani, S.; Huss, M.; Nielsen, J.; Ponten, F.; Uhlen, M., Analysis of the Human Tissue-specific Expression by Genome-wide Integration of Transcriptomics and Antibody-based Proteomics. *Molecular & Cellular Proteomics* **2014,** *13* (2), 397-406.

43. Yang, Z. N.; Bosron, W. F.; Hurley, T. D. Structure of human chi chi alcohol dehydrogenase: A glutathione-dependent formaldehyde dehydrogenase. *J Mol Biol* **265:**330-343; 1997.

44. Barnett, S. D.; Buxton, I. L. O., The Role of S-nitrosoglutathione Reductase (GSNOR) in Human Disease and Therapy. *Crit Rev Biochem Mol Biol* **2017,** *52* (3), 340- 354.

45. Sanghani, P. C.; Davis, W. I.; Zhai, L.; Robinson, H., Structure-Function Relationships in Human Glutathione-Dependent Formaldehyde Dehydrogenase. Role of Glu-67 and Arg-368 in the Catalytic Mechanism. *Biochemistry* **2006,** *45*, 4819-4830.

46. Kubienová, L.; Kopecný, D.; Tylichová, M.; Briozzo, P.; Skopalová, J.; Sebela, M.; Navrátil, M.; Tâche, R.; Luhová, L.; Barroso, J. B.; Petrivalský, M., Structural and functional characterization of a plant S-nitrosoglutathione reductase from Solanum lycopersicum. *Biochimie* **2013,** *95* (4), 889-902.

47. Auld, D. S.; Bergman, T. The role of zinc for alcohol dehydrogenase structure and function. *Cell Mol Life Sci* **65:**3961-3970; 2008.

48. Jelokova, J.; Karlsson, C.; Estonius, M.; Jornvall, H.; Hoog, J. O. Features of Structural Zinc in Mammalian Alcohol-Dehydrogenase - Site-Directed Mutagenesis of the Zinc Ligands. *Eur J Biochem* **225:**1015-1019; 1994.

49. Adinolfi, A.; Adinolfi, M.; Hopkinson, D. A. Immunological and Biochemical-Characterization of the Human Alcohol-Dehydrogenase Chi-Adh Isozyme. *Annals of Human Genetics* **48:**1-10; 1984.

50. Estonius, M.; Svensson, S.; Hoog, J. O. Alcohol dehydrogenase in human tissues: Localisation of transcripts coding for five classes of the enzyme. *Febs Lett* **397:**338-342; 1996.

51. Jensen, D. E.; Belka, G. K.; Du Bois, G. C. S-Nitrosoglutathione is a substrate for rat alcohol dehydrogenase class III isoenzyme. *Biochem J* **331 (Pt 2):**659-668; 1998.

52. Thompson, C. M.; Ceder, R.; Grafstrom, R. C. Formaldehyde dehydrogenase: Beyond phase I metabolism. *Toxicol Lett* **193:**1-3; 2010.

53. Staab, C. A.; Hellgren, M.; Hoog, J. O. Dual functions of alcohol dehydrogenase 3: implications with focus on formaldehyde dehydrogenase and S-nitrosoglutathione reductase activities. *Cell Mol Life Sci* **65:**3950-3960; 2008.

54. Godoy, L.; Gonzalez-Duarte, R.; Albalat, R. S-nitrosogluthathione reductase activity of amphioxus ADH3: insights into the nitric oxide metabolism. *Int J Biol Sci* **2:**117-124; 2006.

55. Kubienova, L.; Ticha, T.; Jahnova, J.; Luhova, L.; Petrivalsky, M. S-Nitrosoglutathione Reductase: The Key Enzyme Regulator of S-nitrosylation. *Chem Listy* **107:**202-208; 2013.

56. Jensen, D. E.; Belka, G. K.; Du Bois, G. C. S-Nitrosoglutathione is a substrate for rat alcohol dehydrogenase class III isoenzyme. *Biochem J* **331 (Pt 2):**659-668; 1998.

57. Koivusalo, M.; Baumann, M.; Uotila, L. Evidence for the identity of glutathione-dependent formaldehyde dehydrogenase and class III alcohol dehydrogenase. *Febs Lett* **257:**105-109; 1989.

58. Jones, D. P.; Thor, H.; Andersson, B.; Orrenius, S. Detoxification Reactions in Isolated Hepatocytes - Role of Glutathione Peroxidase, Catalase, and Formaldehyde Dehydrogenase in Reactions Relating to N-Demethylation by Cytochrome-P-450 System. *J Biol Chem* **253:**6031-6037; 1978.

59. Sanghani, P. C.; Stone, C. L.; Ray, B. D.; Pindel, E. V.; Hurley, T. D.; Bosron, W.F.

Kinetic mechanism of human glutathione-dependent formaldehyde dehydrogenase. *Biochemistry-Us* **39:**10720-10729; 2000.

60. Hedberg, J. J.; Hoog, J. O.; Nilsson, J. A.; Xi, Z.; Elfwing, A.; Grafstrom, R. C. Expression of alcohol dehydrogenase 3 in tissue and cultured cells from human oral mucosa. *Am J Pathol* **157:**1745-1755; 2000.

61. Teng, S.; Beard, K.; Pourahmad, J.; Moridani, M.; Easson, E.; Poon, R.; O'Brien, P. J. The formaldehyde metabolic detoxification enzyme systems and molecular cytotoxic mechanism in isolated rat hepatocytes. *Chem-Biol Interact* **130:**285-296; 2001.

62. Thrasher, J. D.; Kilburn, K. H. Embryo toxicity and teratogenicity of formaldehyde. *Arch Environ Health* **56:**300-311; 2001.

63. Iborra, F. J.; Renaupiqueras, J.; Portoles, M.; Boleda, M. D.; Guerri, C.; Pares, X. Immunocytochemical and Biochemical Demonstration of Formaldehyde Dehydrogenase (Class-Iii Alcohol-Dehydrogenase) in the Nucleus. *J Histochem Cytochem* **40:**1865- 1878; 1992.

64. Hedberg, J. J.; Griffiths, W. J.; Nilsson, S. J. F.; Höög, J.-O., Reduction of S-nitrosoglutathione by human alcohol dehydrogenase 3 is an irreversible reaction as analysed by electrospray mass spectrometry. *Eur J Biochem* **2003,** *270* (6), 1249-2156.

65. Williamson, D. H.; Lund, P.; Krebs, H. A. Redox State of Free Nicotinamide-Adenine Dinucleotide in Cytoplasm and Mitochondria of Rat Liver. *Biochem J*

103:514-+; 1967.

66. Staab, C. A.; Hellgren, M.; Hoog, J. O. Dual functions of alcohol dehydrogenase 3: implications with focus on formaldehyde dehydrogenase and S-nitrosoglutathione reductase activities. *Cell Mol Life Sci* **65:**3950-3960; 2008.

67. Liu, L.; Yan, Y.; Zeng, M.; Zhang, J.; Hanes, M. A.; Ahearn, G.; McMahon, T. J.; Dickfeld, T.; Marshall, H. E.; Que, L. G.; Stamler, J. S. Essential roles of S-nitrosothiols in vascular homeostasis and endotoxic shock. *Cell* **116:**617-628; 2004.

68. Barnett, S. D. and I. L. O. Buxton (2017). "The role of S-nitrosoglutathione reductase (GSNOR) in human disease and therapy." Crit Rev Biochem Mol Biol **52**(3): 340-354.

69. Que, L. G., et al. (2009). "S-nitrosoglutathione reductase: an important regulator in human asthma." Am J Respir Crit Care Med **180**(3): 226-231.

70. Spadaro, D., et al. (2010). "The redox switch: dynamic regulation of protein function by cysteine modifications." Physiol Plant **138**(4): 360-371.

71. Staab, C. A., et al. (2008). "Reduction of S-nitrosoglutathione by alcohol dehydrogenase 3 is facilitated by substrate alcohols via direct cofactor recycling and leads to GSH-controlled formation of glutathione transferase inhibitors." Biochem J **413**(3): 493-504.

72. Hess, D. T. and J. S. Stamler (2012). "Regulation by S-nitrosylation of protein post-translational modification." J Biol Chem **287**(7): 4411-4418.

73. Fernandez, M. R., et al. (2003). "S-nitrosoglutathione reductase activity of human

and yeast glutathione-dependent formaldehyde dehydrogenase and its nuclear and cytoplasmic localisation." <u>Cell Mol Life Sci</u> **60**(5): 1013-1018.

74. Miersch, S. and B. Mutus (2005). "Protein S-nitrosation: biochemistry and characterization of protein thiol-NO interactions as cellular signals." <u>Clin Biochem</u> **38**(9): 777-791.

75. Jahnova, J., et al. (2019). "S-Nitrosoglutathione Reductase-The Master Regulator of Protein S-Nitrosation in Plant NO Signaling." <u>Plants (Basel)</u> **8**(2).

76. Cohn, L.; Elias, J. A.; Chupp, G. L. ASTHMA: Mechanisms of disease persistence and progression. *Annu Rev Immunol* **22:**789-815; 2004.

77. Bobadilla, J. L.; Macek, M. J.; Fine, J. P.; Farrell, P. M., Cystic fibrosis: A worldwide analysis of CFTR mutations—correlation with incidence data and application to screening. *Hum Mutat* **2002,** *19* (6), 575-606.

78. Green, L. S.; Chun, L. E.; Patton, A. K.; Sun, X.; Rosenthal, G. J.; Richards, J. P., Mechanism of Inhibition for N6022, a First-in-Class Drug Targeting S-Nitrosoglutathione Reductase. *Biochemistry* **2012,** *51*, 2157-2168.

79. Fontana, K. Studies on Nitric Oxide Generation and its Enzymatic Degradation. Electronic Theses and Dissertations*,* 2018

80. Hart, T. W. (1985) Some Observations Concerning the S-Nitroso and S-Phenylsulfonyl Derivatives of L-Cysteine and Glutathione. *Tetrahedron Lett* **26**, 2013-2016

81. Jensen, D. E.; Belka, G. K.; Du Bois, G. C. S-Nitrosoglutathione is a substrate for

rat alcohol dehydrogenase class III isoenzyme. Biochem J 331 (Pt 2):659-668; 1998.

82. Geddes, C., Parfenov, A., Roll, D., Uddin, M., & Lakowicz, J. (2003). Fluorescence Spectral Properties of Indocyanine Green on a Roughened Platinum Electrode: Metal-Enhanced Fluorescence. *Journal Of Fluorescence*, *13*(6), 453-457. doi: 10.1023/b:jofl.0000008055.22336.0b

83. Sjöback, R., Nygren, J., & Kubista, M. (1995). Absorption and fluorescence properties of fluorescein. *Spectrochimica Acta Part A: Molecular And Biomolecular Spectroscopy*, *51*(6), L7-L21. doi: 10.1016/0584-8539(95)01421-p

84. Johnson, M. (2011). FITC/Fluorescein. *Materials And Methods*, *1*. doi: 10.13070/mm.en.1.189

85. Sun, B. L., Palmer, L., Alam, S. R., Adekoya, I., Brown-Steinke, K., Periasamy, A., and Mutus, B. (2017) O-Aminobenzoyl-S-nitrosoglutathione: A fluorogenic, cell permeable, pseudo-substrate for S-nitrosoglutathione reductase. *Free Radic Biol Med* **108**, 445-451

86. Hart, T. W. (1985) Some Observations Concerning the S-Nitroso and S-Phenylsulfonyl Derivatives of L-Cysteine and Glutathione. *Tetrahedron Lett* **26**, 2013-2016

87. Ellman, G. L. (1958) A colorimetric method for determining low concentrations of mercaptans. *Arch Biochem Biophys* **74**, 443-450

88. Raturi, A., Miersch, S., Hudson, J. W., and Mutus, B. (2008) Platelet microparticle-

associated protein disulfide isomerase promotes platelet aggregation and inactivates insulin. *Biochim Biophys Acta* **1778**, 2790-2796

89. Root, P., Sliskovic, I., and Mutus, B. (2004) Platelet cell-surface protein disulphide-isomerase mediated S-nitrosoglutathione consumption. *Biochem J* **382**, 575-580

90. Liu, H., Chen, J., Li, W., Rose, M. E., Shinde, S. N., Balasubramani, M., Uechi, G. T., Mutus, B., Graham, S. H., and Hickey, R. W. (2015) Protein disulfide isomerase as a novel target for cyclopentenone prostaglandins: implications for hypoxic ischemic injury. *FEBS J* **282**, 2045-2059

91. Zai, A., Rudd, M. A., Scribner, A. W., and Loscalzo, J. (1999) Cell-surface protein disulfide isomerase catalyzes transnitrosation and regulates intracellular transfer of nitric oxide. *J Clin Invest* **103**, 393-399

92. Pan, S., Chen, H. H., Correia, C., Dai, H., Witt, T. A., Kleppe, L. S., Burnett, J. C., Jr., and Simari, R. D. (2014) Cell surface protein disulfide isomerase regulates natriuretic peptide generation of cyclic guanosine monophosphate. *PLoS One* **9**, e112986

93. Kallakunta, V. M., Slama-Schwok, A., and Mutus, B. (2013) Protein disulfide isomerase may facilitate the efflux of nitrite derived S-nitrosothiols from red blood cells. *Redox Biol* **1**, 373-380

94. Prado, G. N., Romero, J. R., and Rivera, A. (2013) Endothelin-1 receptor antagonists regulate cell surface-associated protein disulfide isomerase in sickle cell disease. *FASEB J* **27**, 4619-4629

95. Wan, S. W., Lin, C. F., Lu, Y. T., Lei, H. Y., Anderson, R., and Lin, Y. S. (2012) Endothelial cell surface expression of protein disulfide isomerase activates beta1 and beta3 integrins and facilitates dengue virus infection. *J Cell Biochem* **113**, 1681-1691

96. Vallon, M., Aubele, P., Janssen, K. P., and Essler, M. (2012) Thrombin-induced shedding of tumour endothelial marker 5 and exposure of its RGD motif are regulated by cell-surface protein disulfide-isomerase. *Biochem J* **441**, 937-944

97. Bi, S., Hong, P. W., Lee, B., and Baum, L. G. (2011) Galectin-9 binding to cell surface protein disulfide isomerase regulates the redox environment to enhance T-cell migration and HIV entry. *Proc Natl Acad Sci U S A* **108**, 10650-10655

98. Zhang, L. M., St Croix, C., Cao, R., Wasserloos, K., Watkins, S. C., Stevens, T., Li, S., Tyurin, V., Kagan, V. E., and Pitt, B. R. (2006) Cell-surface protein disulfide isomerase is required for transnitrosation of metallothionein by S-nitroso-albumin in intact rat pulmonary vascular endothelial cells. *Exp Biol Med (Maywood)* **231**, 1507-1515

99. Sliskovic, I., Raturi, A., and Mutus, B. (2005) Characterization of the S-denitrosation activity of protein disulfide isomerase. *J Biol Chem* **280**, 8733-8741

100. Akhter, S., Green, J. R., Root, P., Thatcher, G. J., and Mutus, B. (2003) Peroxynitrite and NO+ donors form colored nitrite adducts with sinapinic acid: potential applications. *Nitric Oxide* **8**, 214-221

101. Chen, X., Wen, Z., Xian, M., Wang, K., Ramachandran, N., Tang, X., Schlegel, H. B., Mutus, B., and Wang, P. G. (2001) Fluorophore-labeled S-nitrosothiols. *J Org*

Chem **66**, 6064-6073

102. Ramachandran, N., Jacob, S., Zielinski, B., Curatola, G., Mazzanti, L., and Mutus, B. (1999) N-dansyl-S-nitrosohomocysteine a fluorescent probe for intracellular thiols and S-nitrosothiols. *Biochim Biophys Acta* **1430**, 149-154

103. Ramachandran, N., Root, P., Jiang, X. M., Hogg, P. J., and Mutus, B. (2001) Mechanism of transfer of NO from extracellular S-nitrosothiols into the cytosol by cell-surface protein disulfide isomerase. *Proc Natl Acad Sci U S A* **98**, 9539-9544

104. Nikitovic, D., and Holmgren, A. (1996) S-nitrosoglutathione is cleaved by the thioredoxin system with liberation of glutathione and redox regulating nitric oxide. *J Biol Chem* **271**, 19180-19185

105. Jensen, D. E., Belka, G. K., and Du Bois, G. C. (1998) S-Nitrosoglutathione is a substrate for rat alcohol dehydrogenase class III isoenzyme. *Biochem J* **331 (Pt 2)**, 659-668

106. Liu, L., Hausladen, A., Zeng, M., Que, L., Heitman, J., and Stamler, J. S. (2001) A metabolic enzyme for S-nitrosothiol conserved from bacteria to humans. *Nature* **410**, 490-494

107. Liu, L., Hausladen, A., Zeng, M., Que, L., Heitman, J., Stamler, J. S., and Steverding, D. (2001) Nitrosative stress: protection by glutathione-dependent formaldehyde dehydrogenase. *Redox Rep* **6**, 209-210

108. Bateman, R. L., Rauh, D., Tavshanjian, B., and Shokat, K. M. (2008) Human carbonyl reductase 1 is an S-nitrosoglutathione reductase. *J Biol Chem* **283**, 35756-

35762

109. Klonis, N., and Sawyer, W. H. (1996) Spectral properties of the prototropic forms of fluorescein in aqueous solution. *J Fluoresc* **6**, 147-157

110. Raturi, A., and Mutus, B. (2007) Characterization of redox state and reductase activity of protein disulfide isomerase under different redox environments using a sensitive fluorescent assay. *Free Radic Biol Med* **43**, 62-70

111. Caba, C., Ali Khan, H., Auld, J., Ushioda, R., Araki, K., Nagata, K., and Mutus, B. (2018) Conserved Residues Lys(57) and Lys(401) of Protein Disulfide Isomerase Maintain an Active Site Conformation for Optimal Activity: Implications for Post-Translational Regulation. *Front Mol Biosci* **5**, 18

112. Onukwue, N., Ventimiglia, L., Potter, M., Aljoudi, S. and Mutus, B. (2019). Simple fluorescent reagents for monitoring disulfide reductase and S-nitroso reductase activities in vitro and in live cells in culture. *Methods*.

APPENDIX A – Recombinant GSNOR

		1 MANEVIKCKA	10	20 AVAWEAGKPL
MGSSHHHHHH	*SSGLVPRGSH*			

30 SIEEIEVAPP	40 KAHEVRIKIIA	50 TAVCHTDAY	60 TLSGADPEGC
70 FPVILGHEGA	80 GIVESVGEGV	90 TKLKAGDTVI	100 PLYIPQCGEC
110 KFCLNPKTNL	120 CQKIRVTQGK	130 GLMPDGTSRF	140 TCKGKTILHY
150 MGTSTFSEYT	160 VVADISVAKI	170 DPLAPLDKVC	180 LLGCGISTGY
190 GAAVNTAKLE	200 PGSVCAVFGL	210 GGVGLAVIMG	220 CKVAGASRII
230 GVDINKDKFA	240 RAKEFGATEC	250 INPQDFSKPI	260 QEVLIEMTDG
270 GVDYSFECIG	280 NVKVMRAALE	290 ACHKGWGVSV	300 VVGVAASGEE
310 IATRPFQLVT	320 GRTWKGTAFG	330 GWKSVESVPK	340 LVSEYMSKKI
250 KVDEFVTHNL	360 SFDEINKAFE	370 LMHSGKSIRT	374 VVKI

LEHHHHHH

Figure A.1: Recombinant wild type GSNOR protein sequence. Amino acids are numbered from Met1 to Ile374, excluding the added histidine-tag (italicized).
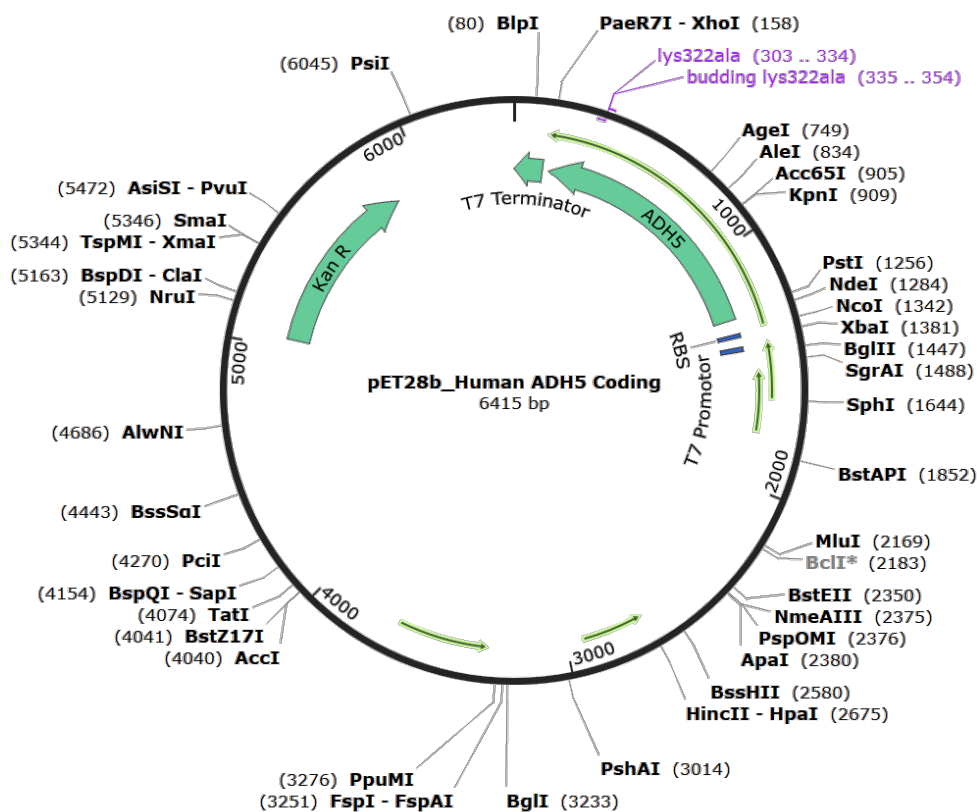
Figure A.2: Recombinant GSNOR Plasmid Map.

The following was designed and performed by Dr Bei Sun.[5] Human ADH5 was purchased from Origene (SC119755) and sub-cloned into the bacterial expression vector pET28b using Cold Fusion Cloning Kit (MJS BioLynx Inc. SYMC010A1). The following primers for PCR were designed according to manufacturer's guidelines:

Forward 5' –GTGCCGCGCGGCAGCCATATGGCGAACGAGGTTATCAAG– 3'

Reverse 5' –GTGGTGGTGGTGGTGCTCGAGAATCTTTACAACAGTTCGAATG– 3'

Colonies were screened using diagnostic restriction enzyme digest and by partial sequencing (Robarts Research Institute, London Regional Genomics Center, London, Ontario, Canada). The final recombinant GSNOR contains a 6X-histidine tag at each terminus.

APPENDIX B – Mass Spectrometry to identify peptides of GSNOR [79]

	1	10	20
MGSSHHHHHH	*SSGLVPRGSH*	MANEVIKCKA	AVAWEAGKPL

30	40	50	60
SIEEIEVAPP	KAHEVRIKIIA	TAVCHTDAY	TLSGADPEGC

70	80	90	100
FPVILGHEGA	GIVESVGEGV	TKLKAGDTVI	PLYIPQCGEC

110	120	130	140
KFCLNPKTNL	CQKIRVTQGK	GLMPDGTSRF	TCKGKTILHY

150	160	170	180
MGTSTFSEYT	VVADISVAKI	DPLAPLDKVC	LLGCGISTGY

190	200	210	220
GAAVNTAKLE	PGSVCAVFGL	GGVGLAVIMG	CKVAGASRII

230	240	250	260
GVDINKDKFA	RAKEFGATEC	INPQDFSKPI	QEVLIEMTDG

270	280	290	300
GVDYSFECIG	NVKVMRAALE	ACHKGWGVSV	VVGVAASGEE

310	320	330	340
IATRPFQLVT	GRTWKGTAFG	GWKSVESVPK	LVSEYMSKKI

250	360	370	374
KVDEFVTHNL	SFDEINKAFE	LMHSGKSIRT	VVKI

LEHHHHHH

Figure B.1 GSNOR Peptide Map

Table B.1: Full peptide list resulting from MS-MS identification. Theoretical amino acid number corresponds to labels beginning at Met1, whereas experimental amino acid numbers include the His tags of the recombinant protein. 292 total amino acids have been sequenced, however only 188 unique amino acids have coverage, resulting in a 52% sequence coverage of the 374 relevant residues. 48% coverage with His tags included.

m/z	Theoretical Amino Acid Number	Experimental Amino Acid Number	Amino Acid Sequence
813.3543	0-6	20-26	(S)HMANEVI(K)
690.0621	7-11	27-33	(I)KCKAAVA/(W)
621.4647	11-22	31-42	(A)/AVAWEAGKPLSI(E)
545.9043	25-43	45-54	(E)/IEVAPPKAHE/(V)
406.9651	35-41	55-61	(E)/VRIKIIA/(T)
457.5103	35-42	55-62	(E)/VRIKIIAT(A)
508.7969	42-56	62-76	(A)/TAVCHTDAYTLSGAD(P)
462.4796	52-56	72-76	(T)LSGAD(P)
762.2355	64-79	84-99	(V)ILGHEGAGIVESVGEG(V)
749.1952	66-81	86-101	(L)/GHEGAGIVESVGEGVT(K)
1260.826	75-87	95-107	(E)/SVGEGVTKLKAGD(T)
1017.545	78-87	98-107	(G)EGVTKLKAGD(T)
889.3751	91-98	111-118	(I)PLYIPQCG(E)
863.8682	131-138	151-158	(F)/TCKGKTIL/(H)
796.6921	139-145	159-165	(L)/HYMGTST(F)
903.3278	187-195	207-215	(T)AKLEPGSVC(A)
646.5185	190-203	210-223	(L)/EPGSVCAVFGLGGV(G)
1091.721	194-205	214-225	(S)VCAVFGLGGVGL/(A)
1074.582	210-220	230-240	(M)GCKVAGASRII(G)
537.7998	211-221	231-241	(G)CKVAGASRIIG(V)
950.457	223-230	243-250	(V)DINKDKFA/(R)
1053.654	228-236	248-256	(D)KFARAKEFG(A)
669.6493	231-242	251-262	(A)/RAKEFGATECIN(P)
726.2026	233-246	253-265	(A)/KEFGATECINPQD(F)
818.1564	239-245	259-265	(T)ECINPQD(F)
1061.054	246-254	266-274	(D)FSKPIQEVL/(I)
1038.94	315-324	335-344	(W)/KGTAFGGWKS(V)
1173.876	320-330	340-350	(F)/GGWKSVESVPK(L)
587.3912	324-334	344-354	(K)SVESVPKLVSE/(Y)
1241.154	334-343	354-363	(S)EYMSKKIKVD(E)
965.4494	353-360	373-380	(F)/DEINKAFE/(L)
1231.957	354-363	374-383	(D)EINKAFELMH(S)

Table B.2: Representative peptide to visualize deuterium uptake.

Peak information: 889.6 m/z, and the amino acid sequence is (I)PLYIPQCG(E) of residues 91-98.

Deuterium uptake (D) and change of deuterium uptake (ΔD) is displayed.

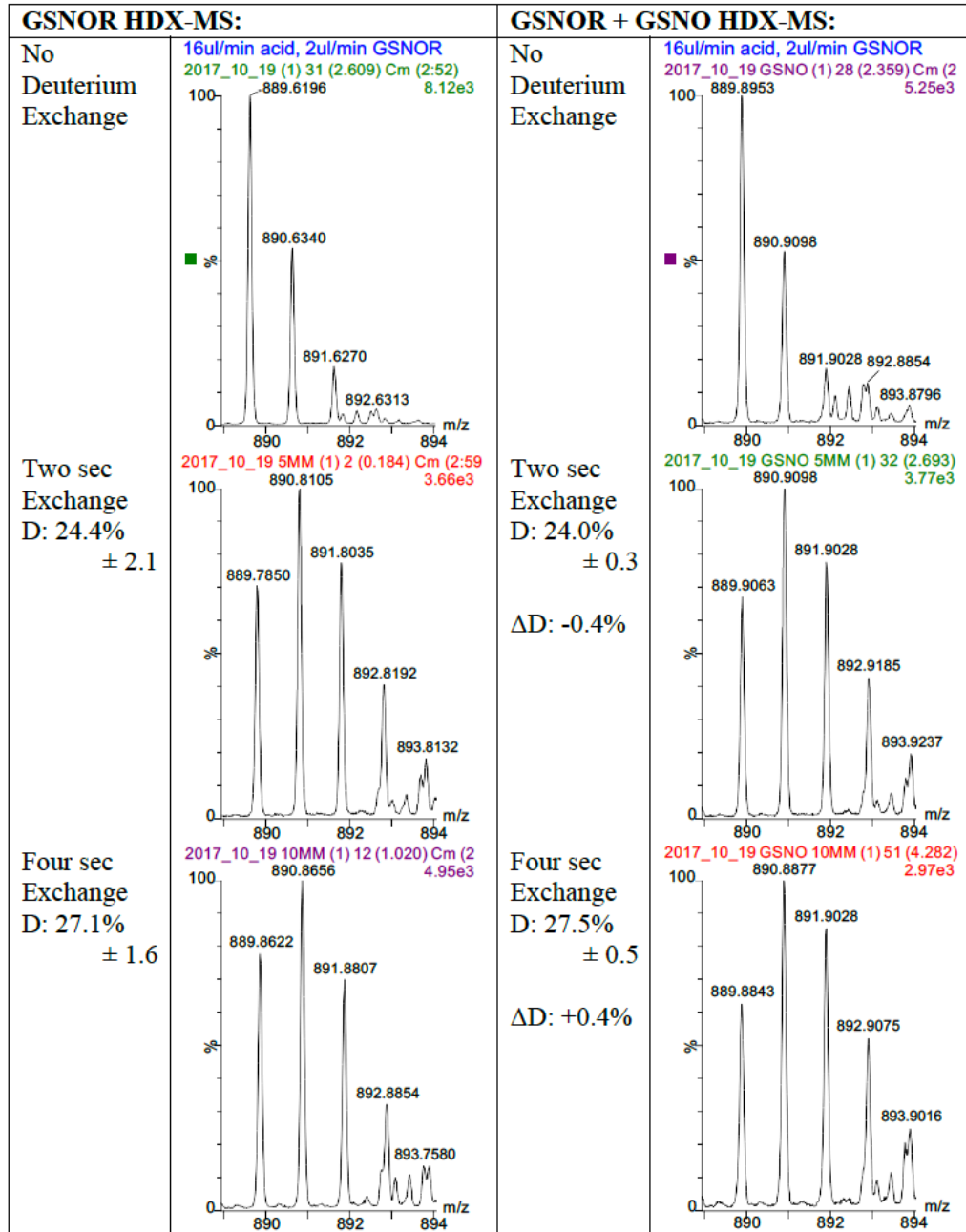| GSNOR HDX-MS:		GSNOR + GSNO HDX-MS:	
No Deuterium Exchange		No Deuterium Exchange	
Two sec Exchange D: 24.4% ± 2.1		Two sec Exchange D: 24.0% ± 0.3 ΔD: -0.4%	
Four sec Exchange D: 27.1% ± 1.6		Four sec Exchange D: 27.5% ± 0.5 ΔD: +0.4%	

Table B.3: Deuterium uptake results of two second reaction time. With and without the addition of substrate GSNO. The difference in those values is shown as a heat map, Red = decrease in deuterium uptake, Blue = increase in uptake. The colour legend used for crystal structure representation images is shown below.
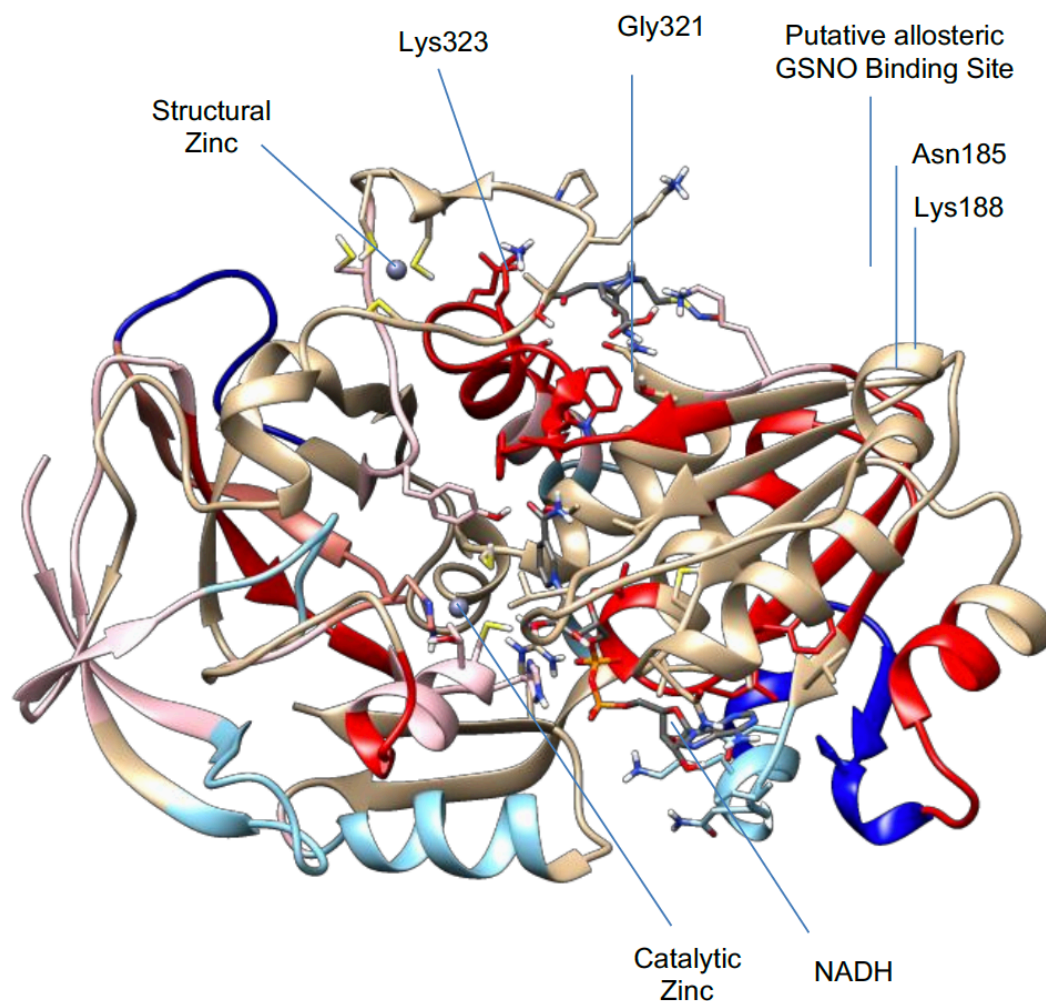
Red	Salmon	Pink		Sky Blue	Blue
-1.8	-0.7	-0.4	0	0.6	3.4

Baseline Deuterium Uptake (%) (n=6)	GSNO Deuterium Uptake (%) (n=2)	Δ Uptake (%) & Colour		Amino Acid Residue	Amino Acid Sequence
17.2 ± 1.4	17.0 ± 0.0	-0.2	Pink	0-6	(S)HMANEVI(K)
15.9 ± 2.7	15.8 ± 1.2	-0.1	Pink	7-11	(I)KCKAAVA/(W)
12.7 ± 1.1	12.8 ± 1.2	+0.2	Sky	11-22	(A)/AVAWEAGKPLSI(E)
17.0 ± 1.2	16.7 ± 0.7	-0.3	Pink	25-34	(E)/IEVAPPKAHE/(V)
21.3 ± 1.6	20.7 ± 0.0	-0.6	Salmon	35-41	(E)/VRIKIIA/(T)
21.6 ± 1.5	20.2 ± 0.5	-1.4	Red	35-42	(E)/VRIKIIAT(A)
11.9 ± 1.1	11.5 ± 0.5	-0.4	Pink	42-56	(A)/TAVCHTDAYTLSGAD(P)
20.3 ± 2.1	19.2 ± 0.5	-1.2	Red	52-56	(T)LSGAD(P)
9.5 ± 0.9	9.2 ± 0.2	-0.3	Pink	64-79	(V)ILGHEGAGIVESVGEG(V)
9.7 ± 0.7	9.0 ± 1.0	-0.7	Salmon	66-81	(L)/GHEGAGIVESVGEGVT(K)
18.4 ± 2.5	20.8 ± 1.2	+2.4	Blue	78-87	(G)EGVTKLKAGD(T)
24.4 ± 2.1	24.0 ± 0.3	-0.4	Pink	91-98	(I)PLYIPQCG(E)
15.7 ± 1.3	15.3 ± 0.0	-0.3	Pink	131-138	(F)/TCKGKTIL/(H)
16.8 ± 1.7	17.0 ± 0.0	+0.3	Sky	139-145	(L)/HYMGTST(F)
25.7 ± 2.8	25.3 ± 0.0	-0.4	Pink	187-195	(T)AKLEPGSVC(A)
19.3 ± 1.6	18.3 ± 1.0	-0.9	Red	190-203	(L)/EPGSVCAVFGLGGV(G)
9.3 ± 0.7	9.0 ± 1.3	-0.3	Pink	194-205	(S)VCAVFGLGGVGL/(A)
16.8 ± 2.5	15.0 ± 0.0	-1.8	Red	210-220	(M)GCKVAGASRII(G)
15.1 ± 1.2	15.3 ± 0.0	+0.2	Sky	223-230	(V)DINKDKFA/(R)
13.4 ± 1.4	12.7 ± 0.7	-0.7	Salmon	228-236	(D)KFARAKEFG(A)
13.8 ± 0.5	15.7 ± 0.0	+1.8	Blue	231-242	(A)/RAKEFGATECIN(P)
19.9 ± 2.3	23.3 ± 0.0	+3.4	Blue	233-245	(A)/KEFGATECINPQD(F)
29.5 ± 3.5	29.7 ± 0.0	+0.1	Sky	239-245	(T)ECINPQD(F)
17.1 ± 1.8	15.8 ± 1.2	-1.2	Red	246-254	(D)FSKPIQEVL/(I)
15.9 ± 2.5	15.0 ± 1.0	-0.9	Red	315-324	(W)/KGTAFGGWKS(V)
13.7 ± 1.3	12.3 ± 0.3	-1.4	Red	320-330	(F)/GGWKSVESVPK(L)
14.8 ± 1.3	14.3 ± 0.3	-0.4	Pink	324-334	(K)SVESVPKLVSE/(Y)
15.0 ± 1.1	15.3 ± 0.0	+0.3	Sky	334-343	(S)EYMSKKIKVD(E)
19.3 ± 1.3	19.0 ± 0.7	-0.3	Pink	353-360	(F)/DEINKAFE/(L)
17.6 ± 1.4	18.2 ± 0.2	+0.6	Sky	354-363	(D)EINKAFELMH(S)

Table B.4: Deuterium uptake results of four second reaction time. With and without the addition of substrate GSNO. The difference in those values is shown as a heat map, Red = decrease in deuterium uptake, Blue = increase in uptake. The colour legend used for crystal structure representation images is shown below.
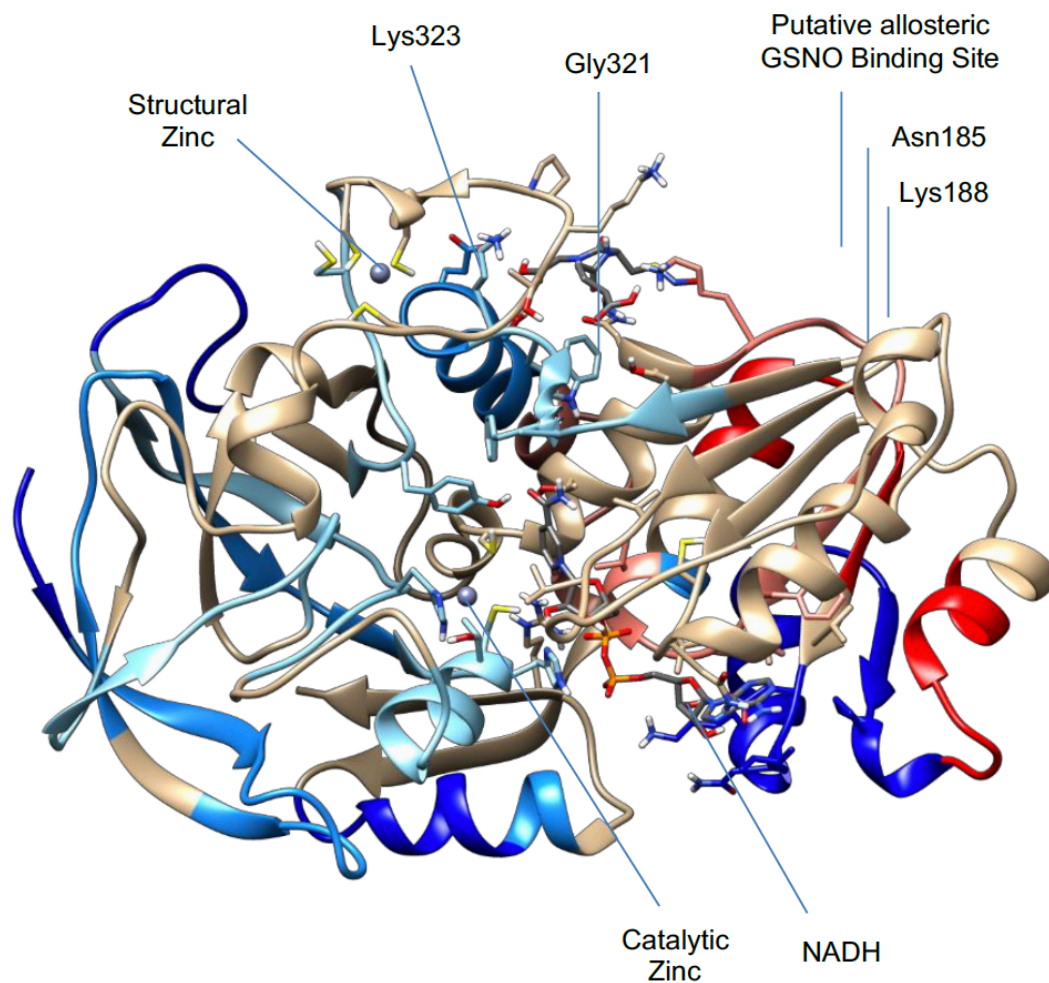
Red	Salmon		Sky Blue	Dodger Blue	Blue
-5.2	-0.8	0	0.7	1.4	5.1

Baseline Deuterium Uptake (%) (n=6)	GSNO Deuterium Uptake (%) (n=2)	Δ Uptake (%) & Colour		Amino Acid Residue	Amino Acid Sequence
16.6 ± 1.8	18.7 ± 0.0	+2.1	Blue	0-6	(S)HMANEVI(K)
16.4 ± 3.1	17.7 ± 0.7	+1.3	Dodger	7-11	(I)KCKAAVA/(W)
12.3 ± 1.9	13.2 ± 0.2	+0.8	Dodger	11-22	(A)/AVAWEAGKPLSI(E)
16.5 ± 2.3	17.7 ± 0.0	+1.2	Dodger	25-34	(E)/IEVAPPKAHE/(V)
20.3 ± 3.1	21.7 ± 0.0	+1.4	Dodger	35-41	(E)/VRIKIIA/(T)
20.4 ± 2.4	21.2 ± 0.5	+0.8	Dodger	35-42	(E)/VRIKIIAT(A)
11.7 ± 2.0	12.2 ± 0.2	+0.5	Sky	42-56	(A)/TAVCHTDAYTLSGAD(P)
20.9 ± 2.5	21.5 ± 0.5	+0.6	Sky	52-56	(T)LSGAD(P)
9.3 ± 1.3	10.0 ± 0.0	+0.7	Sky	64-79	(V)ILGHEGAGIVESVGEG(V)
9.2 ± 1.4	9.5 ± 0.5	+0.3	Sky	66-81	(L)/GHEGAGIVESVGEGVT(K)
19.2 ± 3.7	23.5 ± 3.5	+4.3	Blue	78-87	(G)EGVTKLKAGD(T)
27.1 ± 1.6	27.5 ± 0.5	+0.4	Sky	91-98	(I)PLYIPQCG(E)
15.3 ± 2.3	16.0 ± 0.0	+0.7	Sky	131-138	(F)/TCKGKTIL/(H)
17.3 ± 2.7	17.7 ± 0.0	+0.3	Sky	139-145	(L)/HYMGTST(F)
24.9 ± 2.7	24.3 ± 0.0	-0.6	Salmon	187-195	(T)AKLEPGSVC(A)
19.3 ± 2.4	18.5 ± 1.8	-0.8	Salmon	190-203	(L)/EPGSVCAVFGLGGV(G)
8.8 ± 1.2	9.7 ± 0.7	+0.9	Dodger	194-205	(S)VCAVFGLGGVGL/(A)
17.7 ± 2.3	13.7 ± 0.0	-4.0	Red	210-220	(M)GCKVAGASRII(G)
14.3 ± 2.4	16.3 ± 0.3	+2.1	Blue	223-230	(V)DINKDKFA/(R)
13.1 ± 2.4	13.2 ± 0.2	+0.1	Sky	228-236	(D)KFARAKEFG(A)
11.0 ± 0.3	14.7 ± 0.0	+3.7	Blue	231-242	(A)/RAKEFGATECIN(P)
18.6 ± 4.0	23.7 ± 0.0	+5.1	Blue	233-245	(A)/KEFGATECINPQD(F)
30.1 ± 2.9	30.7 ± 0.0	+0.6	Sky	239-245	(T)ECINPQD(F)
17.4 ± 2.3	12.2 ± 3.8	-5.2	Red	246-254	(D)FSKPIQEVL/(I)
15.8 ± 3.6	15.8 ± 0.2	+0.1	Sky	315-324	(W)/KGTAFGGWKS(V)
13.0 ± 2.0	13.5 ± 0.2	+0.5	Sky	320-330	(F)/GGWKSVESVPK(L)
14.5 ± 1.6	15.3 ± 0.3	+0.8	Dodger	324-334	(K)SVESVPKLVSE/(Y)
15.7 ± 2.2	15.3 ± 0.0	-0.3	Salmon	334-343	(S)EYMSKKIKVD(E)
17.5 ± 2.8	19.7 ± 0.3	+2.2	Blue	353-360	(F)/DEINKAFE/(L)
17.2 ± 2.8	18.2 ± 0.5	+1.0	Dodger	354-363	(D)EINKAFELMH(S)

| Δ Deuterium Uptake (%)					
Red	Salmon	Pink		Sky Blue	Blue
-1.8	-0.7	-0.4	0	0.6	3.4

Figure B1: HDX-MS heat map after two seconds of deuterium exchange. Red conveys a decrease in deuterium incorporation after in inclusion of GSNO, Blue conveys an increase. The putative allosteric binding site with GSNO is shown, along with labels of the implicated resides involved in allosteric binding.

Δ Deuterium Uptake (%)					
Red	Salmon		Sky Blue	Dodger Blue	Blue
-5.2	-0.8	0	0.7	1.4	5.1

Figure B2: HDX-MS heat map after four seconds of deuterium exchange. Red conveys a decrease in deuterium incorporation after in inclusion of GSNO, Blue conveys an increase. The putative allosteric binding site with GSNO is shown, along with labels of the implicated resides involved in allosteric binding.

(i)
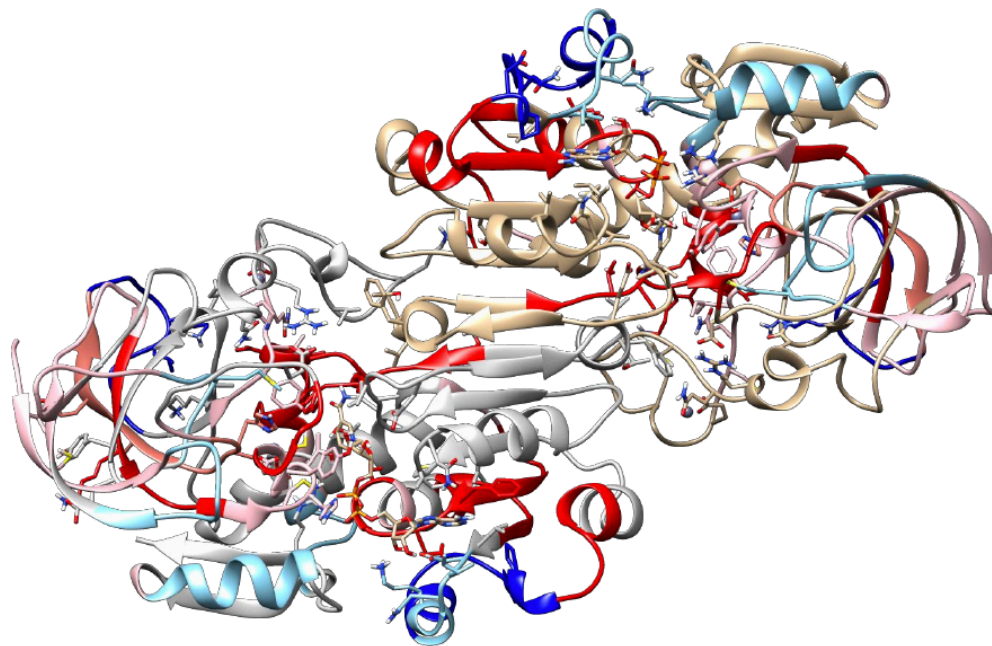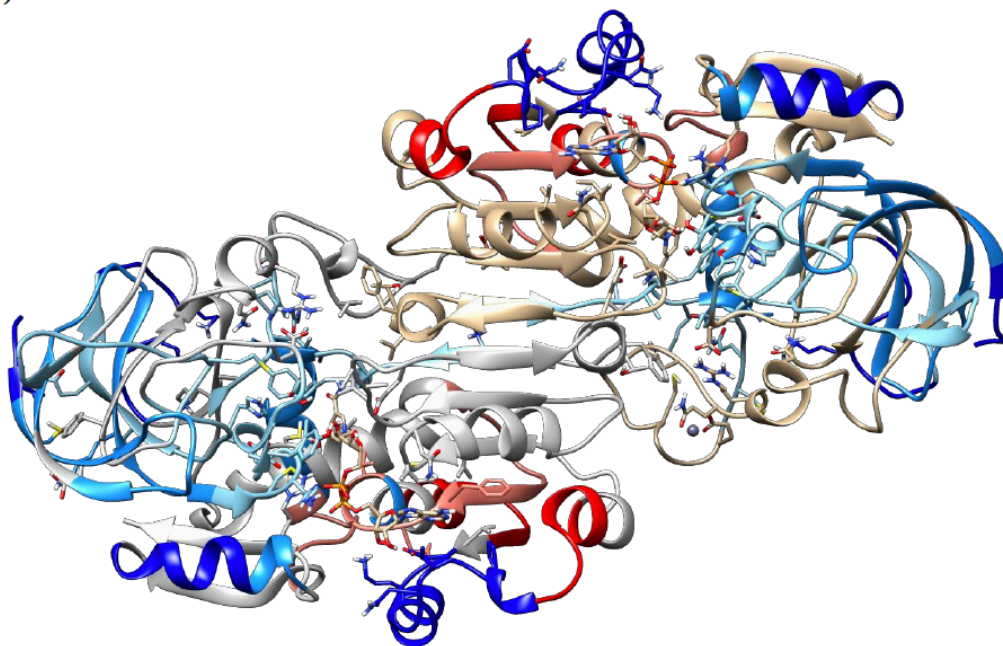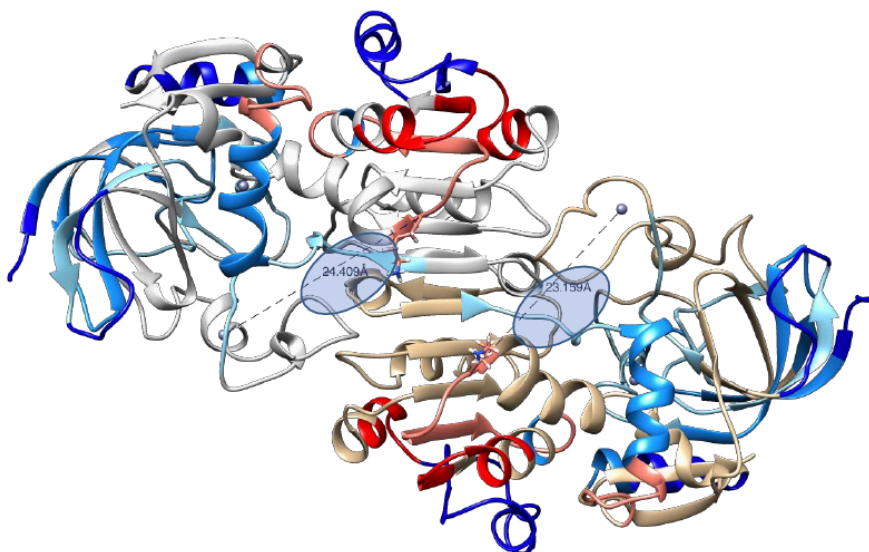

(ii)

Figure B3 (i-ii): HDX-MS heat maps with dimerized GSNOR.

    (i) GSNOR two second reaction data on dimerized structure.

    (ii) GSNOR four second reaction data on dimerized structure.
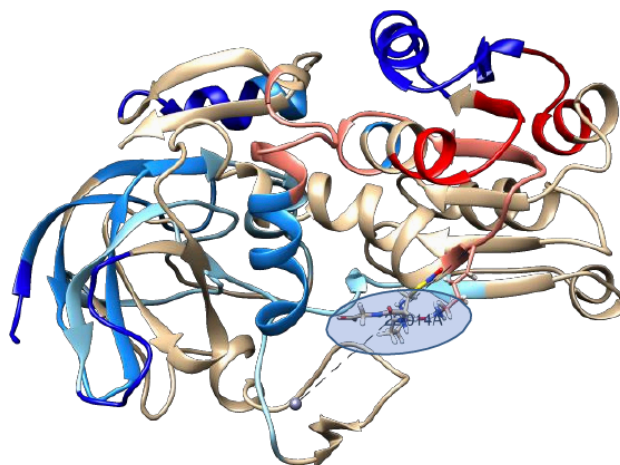
(iii)

(iv)

Figure B3 (iii-iv): HDX-MS heat maps with dimerized GSNOR.

(iii) 'Back-side' view of four second reaction data; 180⁰ horizontal rotation of (ii). Blue circles demonstrate location of allosteric GSNO binding. Blue dashed lines denote the distance between the α-carbon of Lys188 and the structural zinc. The distances are 24.4 Å for the left sided monomer and 23.2 Å for the right.

(iv) Similar orientation of (iii), of the four second reaction data. GSNO is shown; blue dashed lines denote the distance between the α-carbon of Lys188 and the structural zinc, 22.0 Å.

APPENDIX C – Supplementary Data for the development of pseudo-substrate [111]

Table C1: ¹H-NMR chemical shifts for the outlined reagents

Reagents	Chemical Shifts (ppm)
TFSNOG (500 MHz, D20, δ)	2.06 (*m, 2H, Glu, Hβ)
	2.42 (t, 2H, Glu, Hγ)
	3.69 (b, 1H, Glu, Hα)
	3.96 (s, 1H, Gly, Hα)
	4.00 (b, 1H, Cys, Hβ)
	6.73-7.75 (aromatic H of fluoresceinyl protons)
TFHCys2 (500 MHz, D20, δ)	2.29 (m, 1H, HCys, Hα)
	2.73 (m, 2H, HCys, Hβ)
	3.58 (t, 2H, HCys, Hγ)
	6.32-7.57 (aromatic H of fluoresceinyl protons)
TFC2Cys2 (500 MHz, D20, δ)	2.51 (t, 2H, Cys, Hβ)
	3.03 (q, 2H, Cys, Hβ)
	3.78 (t, 1H, Cys, Hα)
	6.46-7.75 (aromatic H of fluoresceinyl protons)

*Abbreviations: δ, chemical shift in parts per million (ppm) downfield from the standard Multiplicities: s, singlet; t, triplet; q, quartet; m, multiplet; b, broadened.

Table C2: ^{1}H-NMR chemical shift for GSNO and AOASNOG (OAbz-GSNO)

^{1}H NMR of GSNO and OAbz-GSNO.

GSNO (500 MHz, D$_2$O, δ)	2.04 (m, 2H, Glu Hβ)
	2.33 (t, 2H, Glu Hγ)
	3.74 (t, 1H, Glu Hα)
	3.84 (s, 1H, Gly Hα)
	3.87 (b, 1H, Cys Hβ)
	4.00 (b, 1H, Cys Hβ)
	4.54 (t, 1H, Cys Hα)
OAbz-GSNO (500 MHz, D$_2$O, δ)	1.94 (m, 1H, Glu Hβ)
	2.12 (m, 1H, Glu Hβ)
	2.28 (t, 2H, Glu Hγ)
	3.55 (s, 2H, Gly Hα)
	3.80 (b, 1H, Cys Hβ)
	3.96 (b, 1H, Cys Hβ)
	4.22 (q, 1H, Glu Hα)
	4.52 (t, 1H, Cys Hα)
	6.75–7.90 (aromatic H)

Abbreviations: δ, chemical shift in parts per million (ppm) downfield from the standard
Multiplicities: s, singlet; t, triplet; q, quartet; m, multiplet; b, broadened
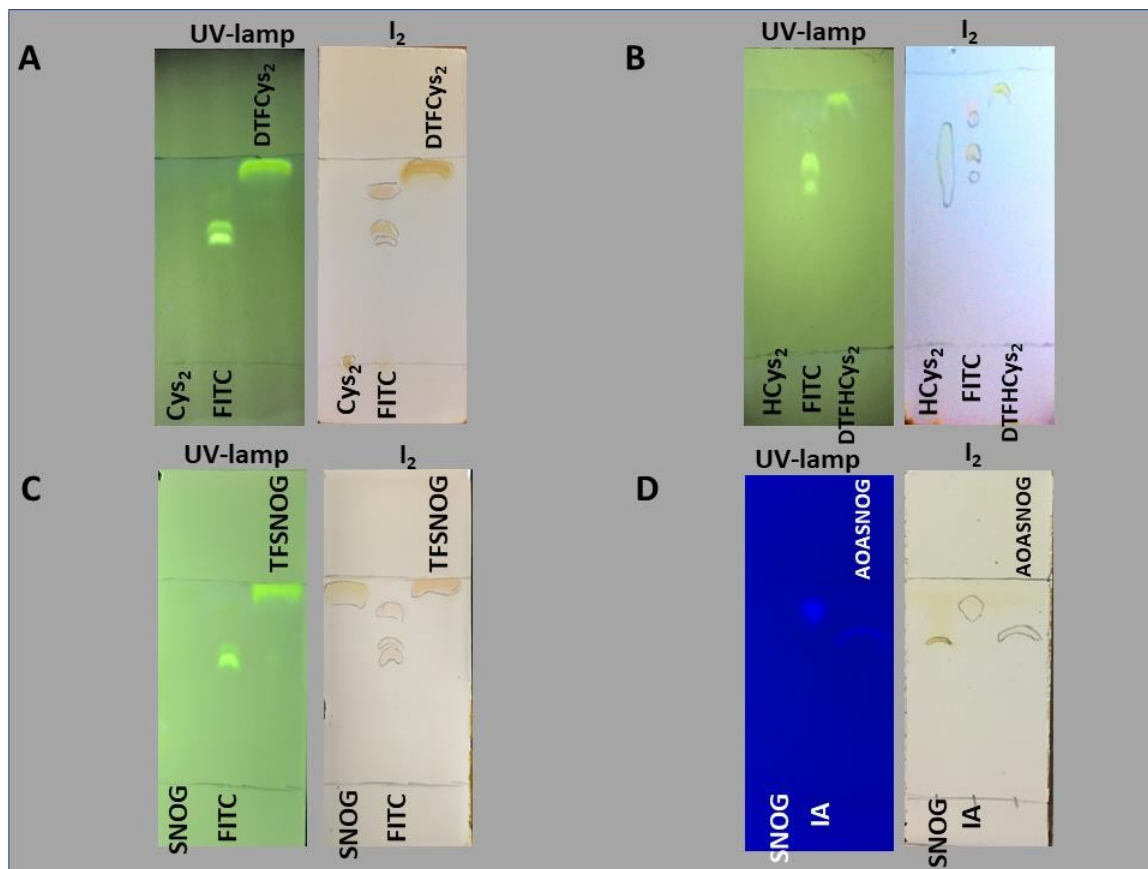
*Figure C1: TLC of starting materials and the products, after purification, visualized by UV lamp (254 nm-plates A, B, C; 366 nm plate D) or I2 vapor. **A**- DTFCys2, **B**- DTFHCys2, **C**-TFSNOG, **D**-AOASNOG. Multiple bands observed in FITC are due to prototropic forms of fluorescein (ref 13 in paper). The mobile phase employed for DTFCys2, DTFHCys2, and TFSNOG was acetone: water: methanol in a 10:10:1. For AOASNOG the mobile phase composition was acetone: water: methanol in a 13:6:1*

VITA AUCTORIS

NAME: Nneamaka Chinwendu Onukwue

PLACE OF BIRTH: Lagos, Nigeria

YEAR OF BIRTH: 1993

EDUCATION: Dowen College, Lagos, Nigeria, 2010

                         Columbia International College, Hamilton, ON, 2011

                         University of Windsor, B.Sc., Windsor, ON, 2017

                         University of Windsor, M.Sc., Windsor, ON, 2019